NAVAL POSTGRADUATE SCHOOL
MONTEREY, CALIFORNIA

THESIS

TURBULENT HEAT FLUX MEASUREMENTS OVER THE GREENLAND, NORWEGIAN AND BARENTS SEAS

by

Joseph C. Johnson

March, 1995

Thesis Co-Advisors: Peter S.Guest
Roland W.Garwood

Approved for public release; distribution is unlimited.

REPORT DOCUMENTATION PAGE

Form Approved OMB No. 0704-0188

1. AGENCY USE ONLY *(Leave blank)*	2. REPORT DATE March 1995	3. REPORT TYPE AND DATES COVERED Master's Thesis

4. TITLE AND SUBTITLE TURBULENT HEAT FLUX MEASUREMENTS OVER THE GREENLAND, NORWEGIAN AND BARENTS SEAS

5. FUNDING NUMBERS

6. AUTHOR(S) Joseph C. Johnson

7. PERFORMING ORGANIZATION NAME(S) AND ADDRESS(ES)
Naval Postgraduate School
Monterey CA 93943-5000

8. PERFORMING ORGANIZATION REPORT NUMBER

9. SPONSORING/MONITORING AGENCY NAME(S) AND ADDRESS(ES)

10. SPONSORING/MONITORING AGENCY REPORT NUMBER

11. SUPPLEMENTARY NOTES The views expressed in this thesis are those of the author and do not reflect the official policy or position of the Department of Defense or the U.S. Government.

12a. DISTRIBUTION/AVAILABILITY STATEMENT
Approved for public release; distribution is unlimited.

12b. DISTRIBUTION CODE

13. ABSTRACT *(maximum 200 words)*

Turbulent heat fluxes in the Greenland, Norwegian and Barents Seas during March 1988, February and March 1989, November 1991 and January and March 1992 have been calculated with the bulk method using shipboard-based measurements of wind speed, air and sea surface temperatures, relative humidity and atmospheric pressure. The largest mean total turbulent heat flux, near 250 W/m^2, was in the Greenland Sea in March 1989. The Norwegian Sea had mean turbulent heat fluxes of 130 W/m^2, whereas the Barents Sea had the smallest mean turbulent heat fluxes. These results compared satisfactorily with climatological studies of the region. However, this study shows the turbulent heat fluxes to be much smaller than those of a recent study, especially in the northern Greenland and Barents Seas. Additionally, comparison of turbulent heat flux values based on 10 minute averages with fluxes calculated from the averages of the bulk variables for an entire ship's cruise (10 - 22 days) shows the values to differ by only ~ 5%.

14. SUBJECT TERMS Turbulent heat flux, Bulk method, Arctic.

15. NUMBER OF PAGES 92

16. PRICE CODE

17. SECURITY CLASSIFICATION OF REPORT	18. SECURITY CLASSIFICATION OF THIS PAGE	19. SECURITY CLASSIFICATION OF ABSTRACT	20. LIMITATION OF ABSTRACT
Unclassified	Unclassified	Unclassified	UL

NSN 7540-01-280-5500

Standard Form 298 (Rev. 2-89)
Prescribed by ANSI Std. 239-18 298-102

Approved for public release; distribution is unlimited.

TURBULENT HEAT FLUX MEASUREMENTS OVER THE
GREENLAND, NORWEGIAN AND BARENTS SEAS

Joseph C. Johnson
Lieutenant , United States Navy
B.S., Eastern Kentucky University, 1985

Submitted in partial fulfillment
of the requirements for the degree of

**MASTER OF SCIENCE IN METEOROLOGY
AND PHYSICAL OCEANOGRAPHY**

from the

NAVAL POSTGRADUATE SCHOOL
March 1995

Author: _____
Joseph C. Johnson

Approved by: _____
Peter S. Guest, Co-Advisor

_____
Roland W. Garwood, Co-Advisor

_____
Robert L. Haney, Chairman
Department of Meteorology

ABSTRACT

Turbulent heat fluxes in the Greenland, Norwegian and Barents Seas during March 1988, February and March 1989, November 1991 and January and March 1992 have been calculated with the bulk method using shipboard-based measurements of wind speed, air and sea surface temperatures, relative humidity and atmospheric pressure. The largest mean total turbulent heat flux, near 250 W/m^2, was in the Greenland Sea in March 1989. The Norwegian Sea had mean turbulent heat fluxes of 130 W/m^2, whereas the Barents Sea had the smallest mean turbulent heat fluxes. These results compared satisfactorily with climatological studies of the region. However, this study shows the turbulent heat fluxes to be much smaller than those of a recent study, especially in the northern Greenland and Barents Seas. Additionally, comparison of turbulent heat flux values based on 10 minute averages with fluxes calculated from averages of the bulk variables for an entire ship's cruise (10 - 22 days) shows the values to differ by only ~ 5%.

TABLE OF CONTENTS

I. INTRODUCTION

Determination of the turbulent (latent plus sensible) heat flux between the ocean and atmosphere is crucial for understanding several aspects of the earth's atmosphere-ocean system. The turbulent heat fluxes combined with the radiative fluxes determine the net exchange of heat across the air-sea interface. It is estimated that deep water formation in the Greenland, Norwegian and Barents Seas comprises about 60% of the total volume of the Arctic Ocean deep water (Swift, Takahashi and Livingston, 1983). Therefore, accurate measurements of the turbulent heat flux in this region are necessary to understand deep oceanic convection and deep water formation.

The measurement of heat flux between the ocean and atmosphere is also an important factor in calculating global circulation of the ocean and atmosphere and therefore is critical to a complete understanding of the global climate. Heat flux is directly linked to oceanic convection and deep water formation in the Arctic. Formation of Arctic deep water causes southerly flow at depth, and the water that sinks is replaced at the surface by the northerly flowing warm surface waters of the North Atlantic. This conveyor belt of oceanic flow is prominent in regulating the global climate. The warming of the ocean surface by the surface currents increases atmospheric instability leading to larger heat fluxes from the ocean to the atmosphere and increased cyclogenesis. The increase in storms causes more precipitation, lower surface salinity, increased ice formation and lower air temperature. As the sea ice melts the surface water becomes more buoyant, and the water column is strongly stratified. The stratification in turn hinders convective overturning, slowing the formation of deep water and completing a negative feedback loop with a cycle of about 20 years (Bourke, 1994).

Knowledge of the amount and variability in time and space of heat flux is also needed to predict the depth and other properties of the atmospheric boundary layer and the oceanic mixed layer. Turbulent heat flux and many properties of the atmospheric boundary layer and the oceanic mixed layer are used in synoptic and mesoscale atmosphere and ocean models. Therefore, accurate measurement of the fluxes offers a chance for improvement in the models. Additionally, an accurate account of heat flux is required to model the formation and dissipation of sea ice properly.

Unfortunately, the Arctic has relatively few observations and is therefore less well understood than the mid-latitudes. Few measurements of sensible and latent heat fluxes have been made over the polar latitudes. Vowinckel and Taylor (1964) (hereafter VT), Bunker (1976) and Gorshkov (1989) have made climotological studies of the turbulent heat fluxes. Additionally, Hakkinen and Cavalieri (1989) (hereafter HC) examined turbulent heat fluxes using gridded Fleet Numerical Meteorology and Oceanography Center (FNMOC), Naval Operational Global Atmospheric Prediction System (NOGAPS) surface analysis for the year 1979. Their results gave extremely high values of total turbulent heat flux near the ice edge in the winter months.

In this study, measurements of the turbulent heat fluxes in the Greenland, Norwegian and Barents Seas were based on direct measurements of bulk variables. Usually, computed fluxes were within the calculated error of the climatological studies. Additionally, comparisons were made with the results of calculating the sensible and latent heat flux based on 10 minute averaged bulk parameters versus ship cruise averaged bulk parameters. These results show the total turbulent heat fluxes are within 5% irrespective of averaging.

In Chapter II, previous studies in the measurement of heat flux in the Greenland, Norwegian and Barents Seas are reviewed. In Chapter III, the data sets and methods of collection are described. Chapter IV contains a description of the bulk formula used to compute the turbulent heat fluxes. The results of this exercise and comparisons with previous studies are included in Chapter V and conclusions are contained in Chapter VI.

II. PREVIOUS STUDIES

In a review of the literature regarding heat flux, four sources were valuable. The first three studies are climatological works, whereas the final study emphasizes the relationship of heat fluxes to numerical ocean and atmosphere modeling. For each study the author's methods, data sources, and assumptions made in the interpretations will be reviewed.

A. VOWINCKEL AND TAYLOR

Vowinckel and Taylor (1964) calculated long wave radiation, latent (evaporation) and sensible heat flux over the Greenland, Norwegian and Barents Seas north of 65° N.

Their calculations are after Sverdrup (1951)

$$E=k(e_s-e_a)\ V \qquad (2.1)$$

$$LHF=E\ L_v \qquad (2.2)$$

where E (mm/24 hrs) is the evaporation rate; k is a dimensionless coefficient called the evaporation factor which is empirically determined from an average for the entire area. VT used 0.104 for k; The parameters e_s (mb) and e_a (mb) are the water vapor pressures at the sea surface and at the shipboard measurement height, respectively; V (m/s) is the wind velocity as measured onboard ship; LHF (cal / cm^2 month) is the latent heat flux; and L_v (cal) is the calculated latent heat of vaporization at that latitude.

VT had more confidence in their measurements of evaporation than of sensible heat flux. Thus, they used the Bowen ratio to calculate sensible heat flux over the water,

$$R=\frac{SHF}{LHF}=0.66\frac{p}{1000}\frac{T_s-T_a}{e_s-e_a} \qquad (2.3)$$

$$SHF=R\ LHF \qquad (2.4)$$

where R is the Bowen ratio; SHF (cal/cm^2 month) is the sensible heat flux; p (mb) is the atmospheric pressure; T_s (C) and T_a (C) are the temperatures of the air and sea surface.

The VT data for wind speed were determined based on ten years of synoptic data at ship M in the Norwegian-Barents Sea. Mean wind speed was based on an evaluation of wind roses published by the British Meteorological Office (1959). Due to the paucity of data, wind speed maps were prepared on a seasonal basis and monthly values were extrapolated. Air and sea surface temperatures were obtained from the British Meteorological Office (1959). Relative humidity, which is needed to compute e_a, was taken from monthly mean maps. The relative humidity maps were produced based on data from ship M, small islands and exposed coastal stations.

The VT flux data are provided for the Norwegian and Greenland Seas in five degree sections of latitude, and no longitudinal distinctions are made. Data were given monthly in units of cal/cm^2 month. Also, the total heat fluxes here are computed by adding the sensible and latent

fluxes. All heat fluxes shown in this thesis are in units of W/m^2. To convert to W/m^2, cal/cm^2 month is multiplied by 0.01614. Tables 2.1, 2.2 and 2.3 are VT heat flux data used for this study.

Month	LHF	SHF	THF
January	59	142	201
February	69	171	240
March	89	206	295

Table 2.1 Latent, sensible and total turbulent heat flux (W/m^2) over the Norwegian-Barents Sea from 80N to 75N (after Vowinckel and Taylor, 1964).

Month	LHF	SHF	THF
January	73	45	118
February	64	60	124
March	90	86	176

Table 2.2 Latent, sensible and total turbulent heat flux (W/m^2) over the Norwegian-Barents Sea from 75N to 70N (after Vowinckel and Taylor, 1964).

Month	LHF	SHF	THF
January	113	44	157
February	84	47	131
March	95	54	149
November	67	32	99

Table 2.3 Latent, sensible and total turbulent heat flux (W/m^2) over the Norwegian-Barents Sea from 70N to 65N (after Vowinckel and Taylor, 1964).

B. GORSHKOV

The World Ocean Atlas edited by Gorshkov (1983), contains annual and monthly maps of the various flux components. The atlas is in Russian with a short summary in English. The Russian headings, captions and other pertinent data were translated by Capt. Mary Lee, USAF.

The main sources of information for compiling the maps were observations at 111 shore stations from 1936 to 1972. The methodology for flux calculations was not stated.

The data were provided as time series depicting annual rates of heat flux for twelve locations in $kcal/cm^2$ year. Station 10 was in the Norwegian-Barents Sea, station 11 was in the Greenland Sea and station 12 in the southern Norwegian Sea (refer to Figure 2.1 for locations; all figures are at the end of chapters). To convert to W/m^2, $kcal/cm^2$ month was multiplied by 16.14. Tables 2.4, 2.5 and 2.6 contain heat flux data germane to this study.

Month	LHF	SHF	THF
January	126	116	242
February	97	97	194
March	73	73	146
November	105	81	186

Table 2.4 Latent, sensible and total turbulent heat flux (W/m^2) at station 10 near 72N/020E over the Norwegian-Barents Sea (after Gorshkov, 1983).

Month	LHF	SHF	THF
January	129	190	319
February	112	161	273
March	100	145	245

Table 2.5 Latent, sensible and total turbulent heat flux (W/m^2) at station 11 near 78N/010E over the Greenland Sea (after Gorshkov, 1983).

Month	LHF	SHF	THF
January	129	186	315
February	113	161	274
March	97	65	162
November	89	61	150

Table 2.6 Latent, sensible and total turbulent heat flux (W/m^2) at station 12 near 64N/005E in the Norwegian Sea (after Gorshkov, 1983).

C. BUNKER

Bunker (1976) computed energy flux over much of the world, including one station in the northern Norwegian and Barents Seas that was useful for this thesis (see Figure 2.1).

Bunker calculated heat flux based on the bulk aerodynamic method. His method used exchange coefficients that vary with wind speed and stability. His equations were in the form

$$LHF = \rho C_E L_v (Q_S - Q_{10}) U_{10} \quad (2.5)$$

$$SHF = \rho C_H C_P (T_S - T_{10}) U_{10} \quad (2.6)$$

where ρ is atmospheric density; C_e and C_h are the variable exchange coefficients for water vapor and sensible heat; C_p is the specific heat constant; Q_s and Q_{10} are the averages of the mixing ratio of air in contact with the surface and at 10 m; U_{10} is the average wind speed at 10 m; and T_s and T_{10} are average temperatures of the sea surface and air at 10 m.

Bunkers' values for the exchange coefficients were obtained from tables calculated from experimental data. The values of the coefficient for water vapor have been applied to the computations of sensible heat, making the coefficients equal.

Bunkers' calculations were based on a National Climatic Center data set, which was collected for the years 1941-1972. Averages for each month of each year for an entire Marsden Square were formed for fluxes and basic meteorological variables. Monthly and annual averages for

the 32-year period were formed for subdivisions of the Marsden Squares. A Norwegian-Barents Sea area was selected at 71 N, 17 E (refer to Figure 2.1 for location). This data set was produced based on 1859 observations over the 32-year period. Table 2.7 portrays the heat flux for this station.

Month	LHF	SHF	THF
January	110	95	205
February	100	90	190
March	100	80	180
November	80	60	140

Table 2.7 Latent, sensible and total turbulent heat flux (W/m^2) over the Norwegian Sea at 71N/017E (after Bunker, 1976).

D. HAKKINEN AND CAVALIERI

Hakkinen and Cavalieri (1989) estimated oceanic surface heat fluxes in the Norwegian, Greenland and Barents Seas using gridded Fleet Numerical Meteorology and Oceanography Center (FNMOC) surface analysis of winds and temperatures for one year. They used the bulk method (Equations 2.2 and 2.3) with the heat (C_h), and moisture (C_q) transfer coefficients fixed at a value 1.5×10^{-3} neglecting any stability dependence. Density was also fixed at 1.3 kg / m^3.

The data for their calculations are based on archived Navy Operational Global Atmospheric Prediction System (NOGAPS) analyses for the period December 1, 1978 through November 30, 1979. The gridded data has a resolution of 250

km. The NOGAPS model data includes sea level pressure, air temperature, vapor pressure, winds and SST. All parameters except SST are given twice daily. SST is given once daily and interpolated to 12 hour intervals for flux computations.

Monthly mean contour plots of total turbulent (sensible and latent) heat fluxes were provided in W/m^2. Tables 2.8 and 2.9 contain total turbulent heat fluxes (LHF + SHF) as interpreted from contoured maps for regions and times corresponding with data analyzed in this thesis.

Month	THF
January	640
February	560
March	420

Table 2.8 Total turbulent heat flux (W/m^2) over the Greenland Sea 77.5N/005E (after Hakkinen and Cavalieri, 1989).

Month	THF
January	150
February	140
March	80
November	140

Table 2.9 Total turbulent heat flux (W/m^2) over the Norwegian Sea 68N/005E (after Hakkinen and Cavalieri, 1989).

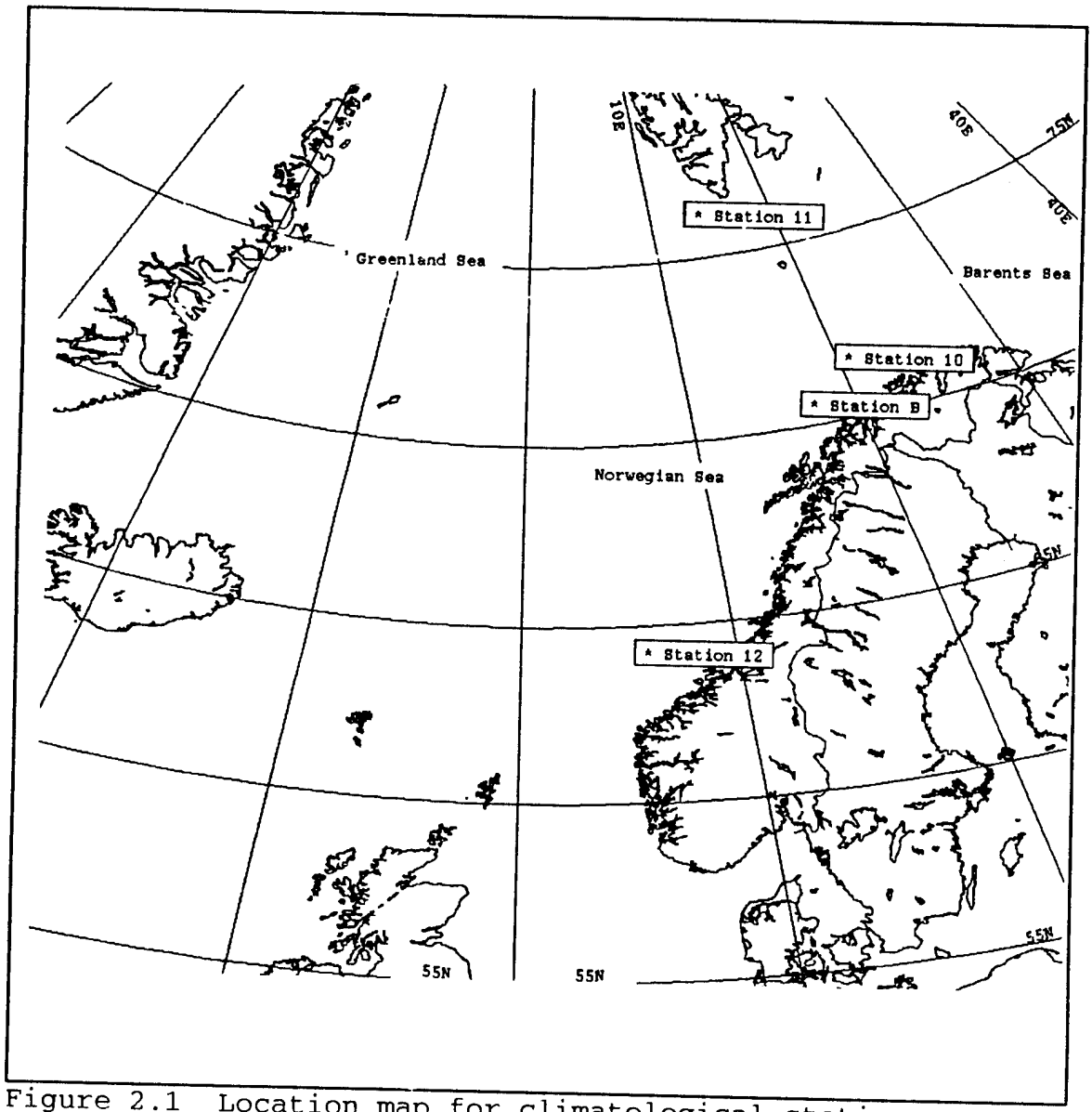

Figure 2.1 Location map for climatological stations. Stations 10, 11 and 12 are data from Gorshkov, and station B is data from Bunker.

III. DATA

A. COLLECTION OF DATA

This study utilizes data collected by Professor Kenneth Davidson and associates at the Naval Postgraduate School (NPS) in the Greenland, Norwegian and Barents Seas during several recent ship cruises (Figure 3.1). A Coastal Climate WeatherPak meteorological station onboard the Research Vessel (R\V) Haakon Mosby sampled air temperature, wind speed and direction relative to the ship's heading every second and relative humidity and atmospheric pressure every 12 seconds. The measurement platform was at 15 m above the sea surface. In addition, the ship's speed and heading were recorded, enabling the calculation of true wind speed and direction. Sea Surface Temperature (SST) was also measured by the ship. All observations were averaged over 10 minute intervals. Details of the various ship cruises are described in later sections.

The temperature data were estimated to be accurate to within 1.0 C and the relative humidity data to within 5%. Wind speeds were estimated to be accurate to within 0.3 m/s. When winds were from the stern, errors are probably greater due to the sheltering effect caused by the ship's superstructure. The measurements of atmospheric pressure are accurate to within 2 millibars.

At times, data were missed or not recorded; during these cases the trends were assumed to be linear and intermediate data points were interpolated.

A common bias involving data collected by ships is storm avoidance. That is, if a ship's crew expects a location to be stormy they will typically avoid that area. This is not so with the cases studied here. In general, the locations and ship tracks were planned in advance and were not significantly deviated from. The only storm avoidance

bias occurred during the later part of SIZEX in January 1992, when an intense cyclone disabled the weather collection unit with winds greater than 28 m/s. This prevented about 24 hours of data collection during a high wind period. This was estimated not to significantly affect the overall heat flux averages.

EXER Sea Date	NORCSEX Norw Mar 88	CEAREX Barents Feb 89	CEAREX Green Mar 89	NORCSEX Norw Nov 91	SIZEX Green Jan 92	SIZEX Barents Mar 92
Wind m/s	7.0 (3.5)	10.7 (3.7)	9.1 (2.7)	9.0 (4.0)	10.8 (5.1)	8.7 (3.3)
Temp C	1.2 (2.1)	-1.4 (3.9)	-9.0 (5.3)	5.8 (2.2)	-5.6 (3.2)	0.1 (3.4)
SST C	5.8 (1.1)	1.8 (0)	1.4 (0)	8.3 (0.5)	1.8 (2.0)	1.8 (3.0)
RH %	68.6 (11.3)	72.0 (12.9)	72.4 (9.6)	69.3 (13.5)	71.7 (11.9)	81.5 (9.7)
Press mb	1002 (8)	997 (8)	991 (11)	999 (14)	996 (12)	1001 (9)

Table 3.1 Mean and standard deviations of input data for indicated exercises.

B. NORCSEX 88

The Norwegian Continental Shelf Exercise (NORCSEX) 88 was a European Research Satellite (ERS-1) pre-launch calibration and validation experiment. The purpose of the ship cruise was to validate data measured by aircraft flown

with ERS-1 sensors. NORCSEX 88 was conducted in the Norwegian Sea and centered around the Norwegian Continental Shelf at 64°30'N and 009°E during March of 1988. From 07 to 18 March, the R/V Haakon Mosby collected meteorological data while transiting along the west coast of Norway (see Figure 3.1 for track). The time series of these data are shown in Figure 3.2.

NORCSEX 88 displayed the lowest wind speeds of all the cases; during the exercise moderate winds prevailed with a mean of only 7.0 m/s. However, gale to storm force conditions occurred on 11 March (Julian day 71); as the wind veered from the south to the north, the wind speed quickly increased to more than 22 m/s. Along with the wind change came a decrease in air temperature and an increase in relative humidity. Throughout the measurement period, the air temperature and sea surface temperature were fairly constant. SST had a range of 2 C to 8 C and a standard deviation of 1.1. Air temperature had a range of -5 C to 5 C and the smallest standard deviation of all the exercises at 2.1 C.

C. CEAREX

The Coordinated Eastern Arctic Exercise (CEAREX) was a large international interdisciplinary project involving several ships, aircraft and ice camps. CEAREX was conducted in the vicinity of the Svalbard Islands from September 1988 to May 1989. For this study, continuous surface measurements collected by the R/V Haakon Mosby from 25 Feb to 23 Mar 1989 were used. From 25 February to 09 March 1989 the ship was in the northern Norwegian and Barents Seas (Figure 3.1). Since these tracks correspond more closely to land and climatological stations in the Barents Sea, this region will be called only the Barents Sea to prevent confusion with locations in the southern Norwegian Sea.

After 10 March, the ship transited on a westerly course to a location west of Svalbard and conducted north-south tracks along the ice edge. Since the measurements in the Barents Sea differed markedly from those in the Greenland Sea, the measurements have been divided into two separate data sets. The time series of data in the Barents Sea is shown in Figure 3.3, and the time series for data in the Greenland Sea is shown in Figure 3.4.

There were several cyclone passages while the ship was located in the Barents Seas. The temperature tended to be near freezing for relatively long periods of time with brief surges of extremely cold air after cyclone passages. The average wind was strong at 10.7 m/s and primarily from the north. Sea surface temperatures were not available for CEAREX. Mean SSTs of 1.8 C and 1.4 C were chosen for CEAREX data in the Barents and Greenland Seas, respectively. These values were based upon averages from SIZEX data along similar tracks and climotological data.

In the Greenland Sea, the air temperatures were much colder than in the Norwegian Sea, with mean temperatures of -9 C compared with -1 C. After passage of a cyclone on about 11 March (Julian day 69) the pressure field was relatively flat with colder temperatures and lower relative humidity.

D. NORCSEX 91

The Norwegian Continental Shelf Exercise (NORCSEX) 91 was a follow-on to NORCSEX 88. Its purpose was a post launch validation of ERS-1 sensors. NORCSEX 91 was conducted in the Norwegian Sea from 08 Nov to 29 Nov 1991. During this period meteorological variables were collected onboard the R/V Haakon Mosby. The time series of data are shown in Figure 3.5.

NORCSEX 91 data contained the warmest air and sea

surface temperatures of all the exercises with means of 5.8 C and 8.3 C, respectively. The temperatures were also less variable than those of other exercises with standard deviations of 2.2 C and 0.5 C. During the period there were several strong cyclones that passed over the ship. These cyclones exhibited higher winds but showed little temperature change.

E. SIZEX

The Seasonal Ice Zone Experiment (SIZEX) was conducted as a part of an ERS-1 ice Synthetic Aperture RADAR (SAR) validation. SIZEX was held in the Greenland Sea during 1992. The experiment has been divided into two periods, one in January and one in March. Time series of data are shown in figures 3.6 and 3.7.

In January, the data were influenced by three prominent cyclone passages. The cyclones were accompanied by strong winds from the south to southeast. The final cyclone, occurring on about 13 January (Julian day 13), was storm force with wind speeds approaching 30 m/s. The storm was strong enough to knock out the weather collection station.

In February and March, there were no intense cyclones but periods with significant winds between 15-20 m/s.

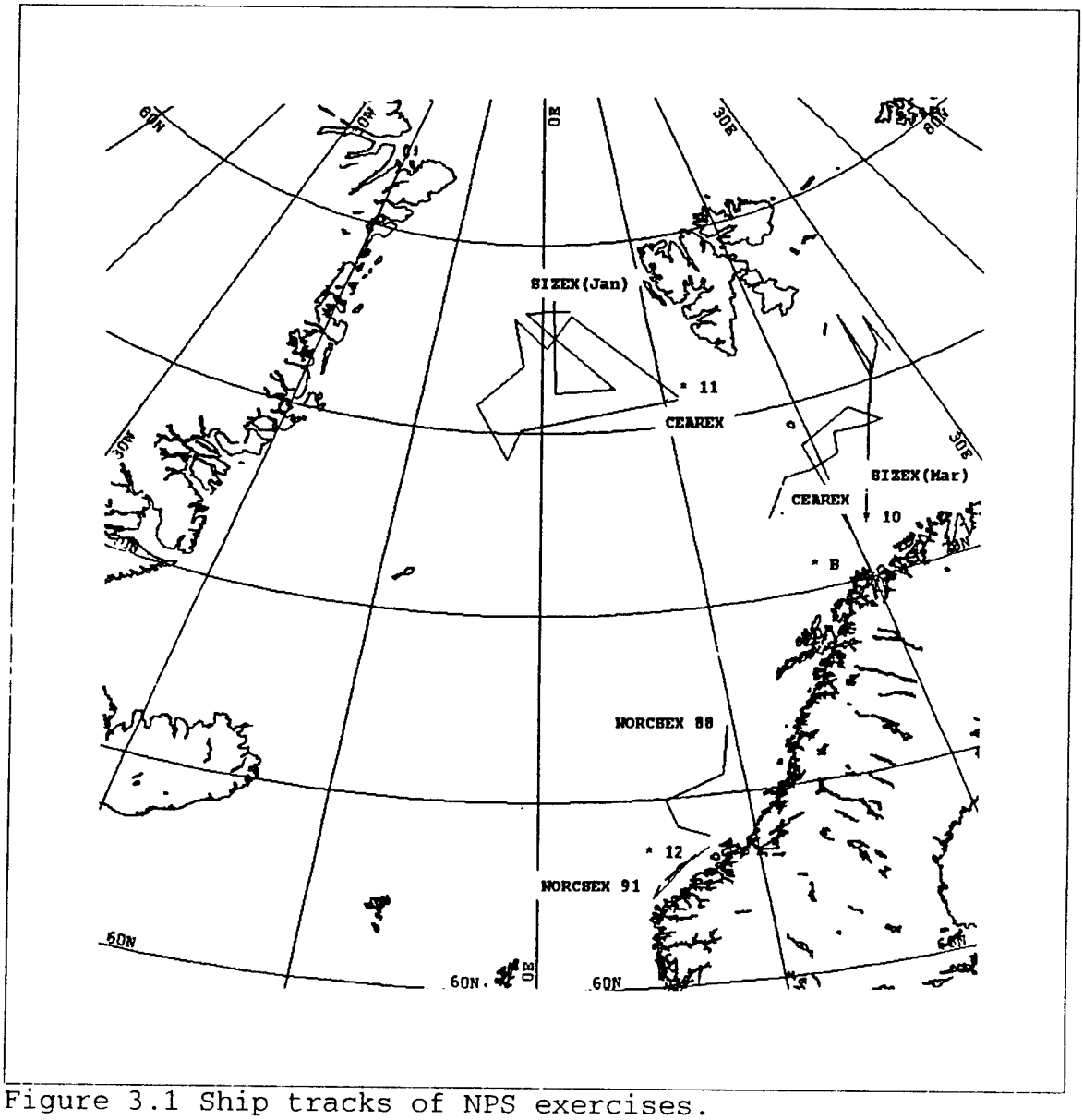

Figure 3.1 Ship tracks of NPS exercises.

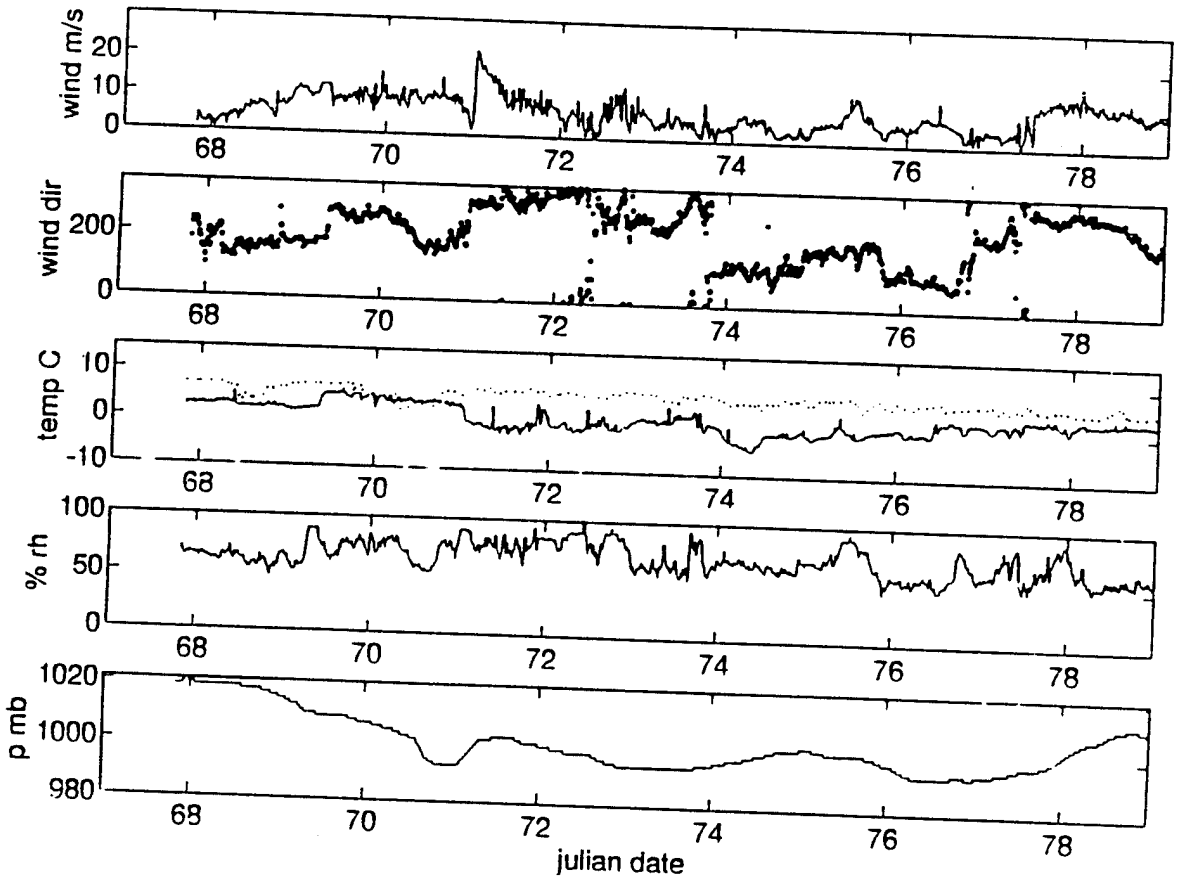

Figure 3.2 Time series of wind speed, wind direction, sea surface temperature (dotted) and air temperature (solid), relative humidity and pressure during NORCSEX88, March 1988.

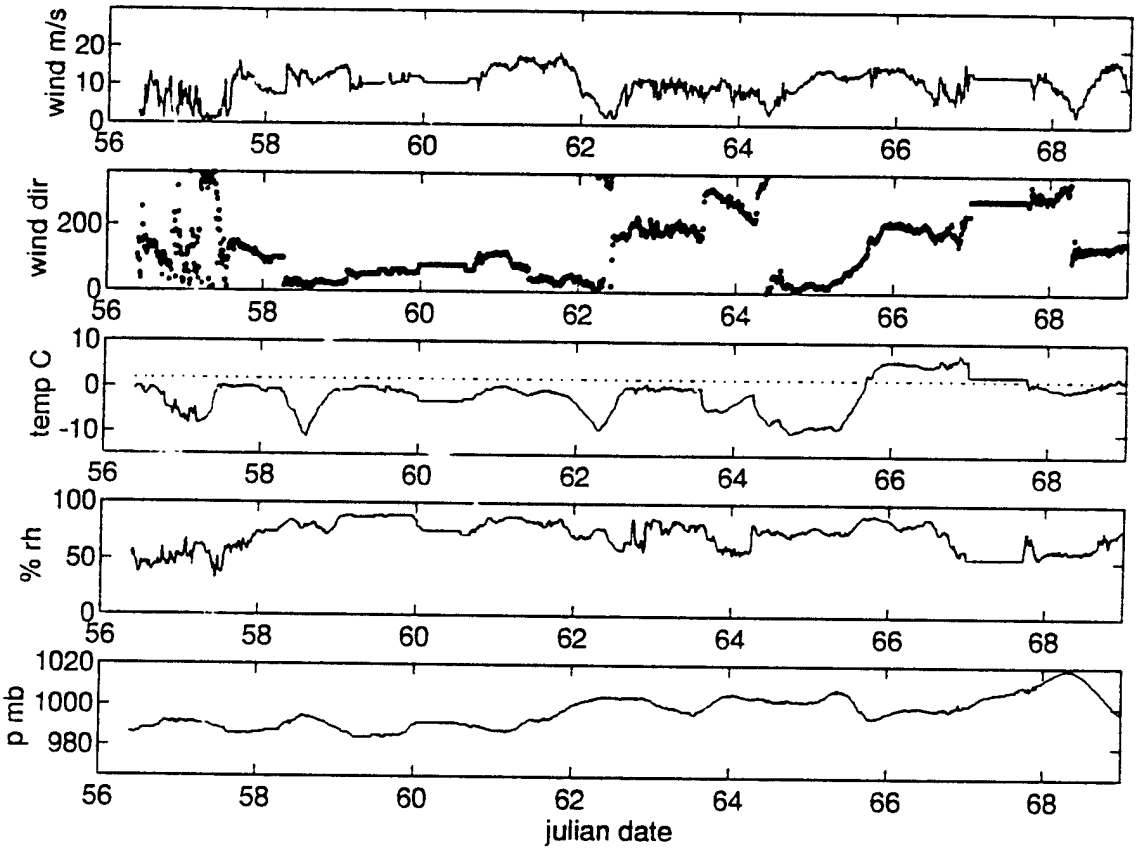

Figure 3.3 Time series of wind speed, wind direction, sea surface temperature (dotted) and air temperature (solid), relative humidity and pressure during CEAREX in the Barents Sea, February-March 1989.

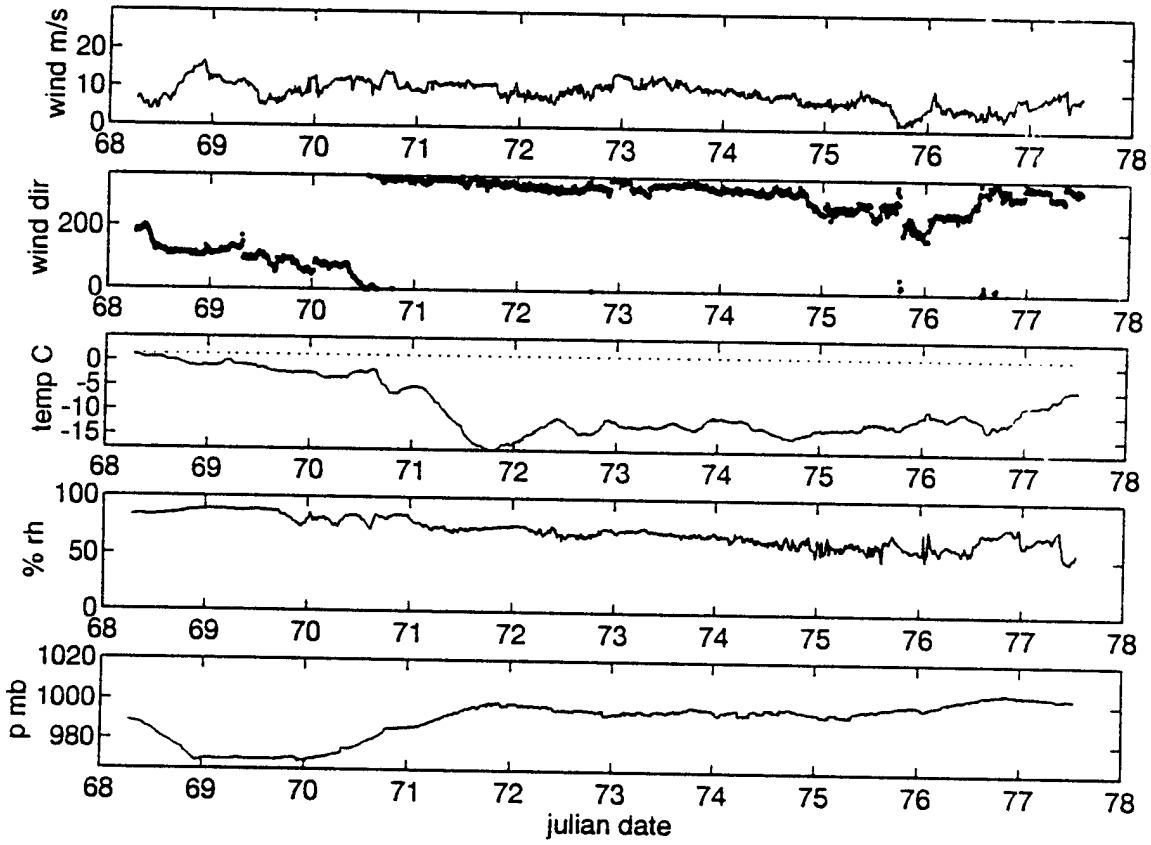

Figure 3.4 Time series of wind speed, wind direction, sea surface temperature (dotted) and air temperature (solid), relative humidity and pressure during CEAREX in the Greenland Sea, March 1989.

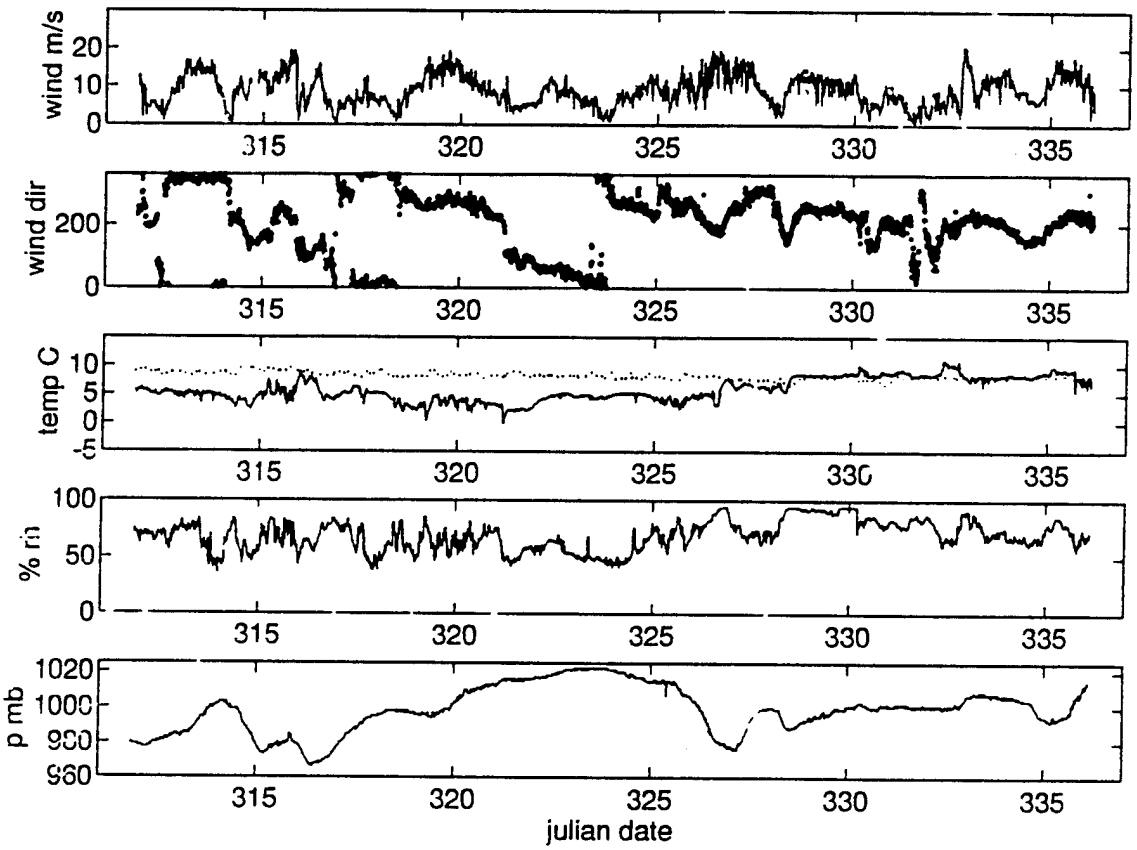

Figure 3.5 Time series of wind speed, wind direction, sea surface temperature (dotted) and air temperature (solid), relative humidity and pressure during NORCSEX91 in the Norwegian Sea, November 1991.

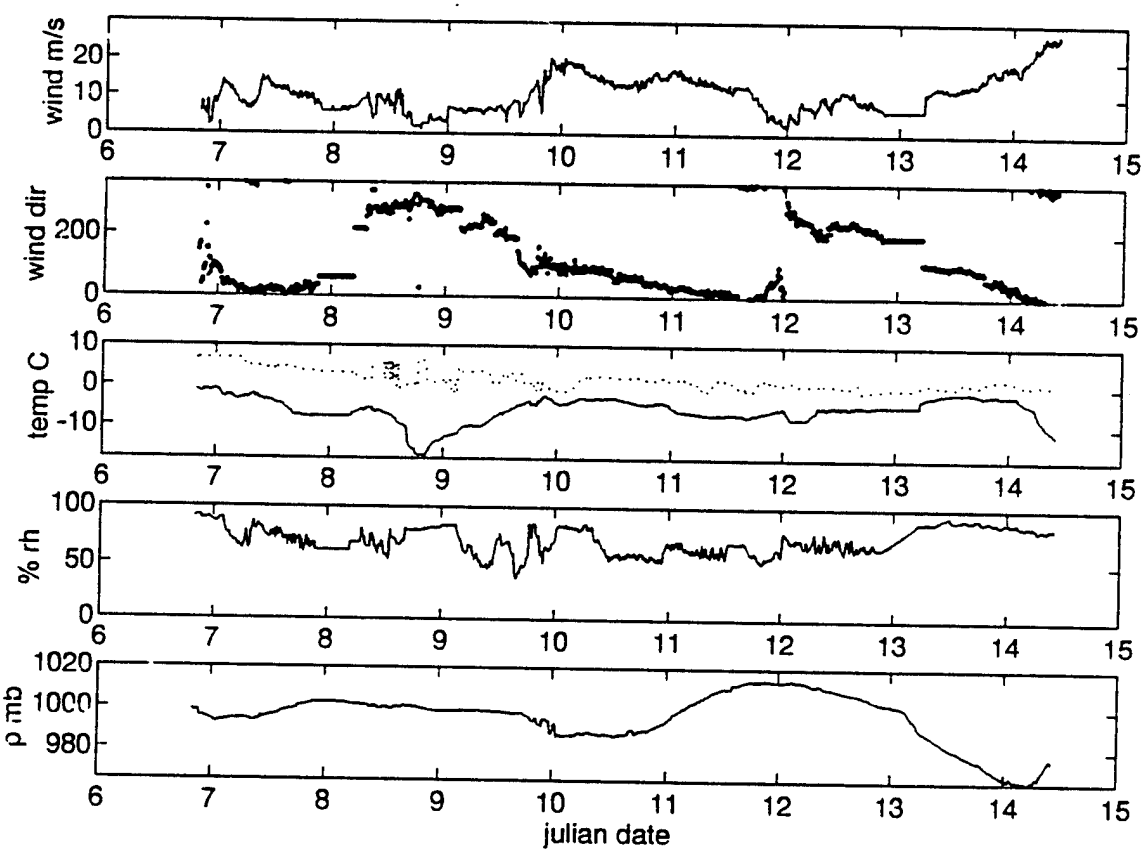

Figure 3.6 Time series of wind speed, wind direction, sea surface temperature (dotted) and air temperature (solid), relative humidity and pressure during SIZEX in the Greenland Sea, January 1992.

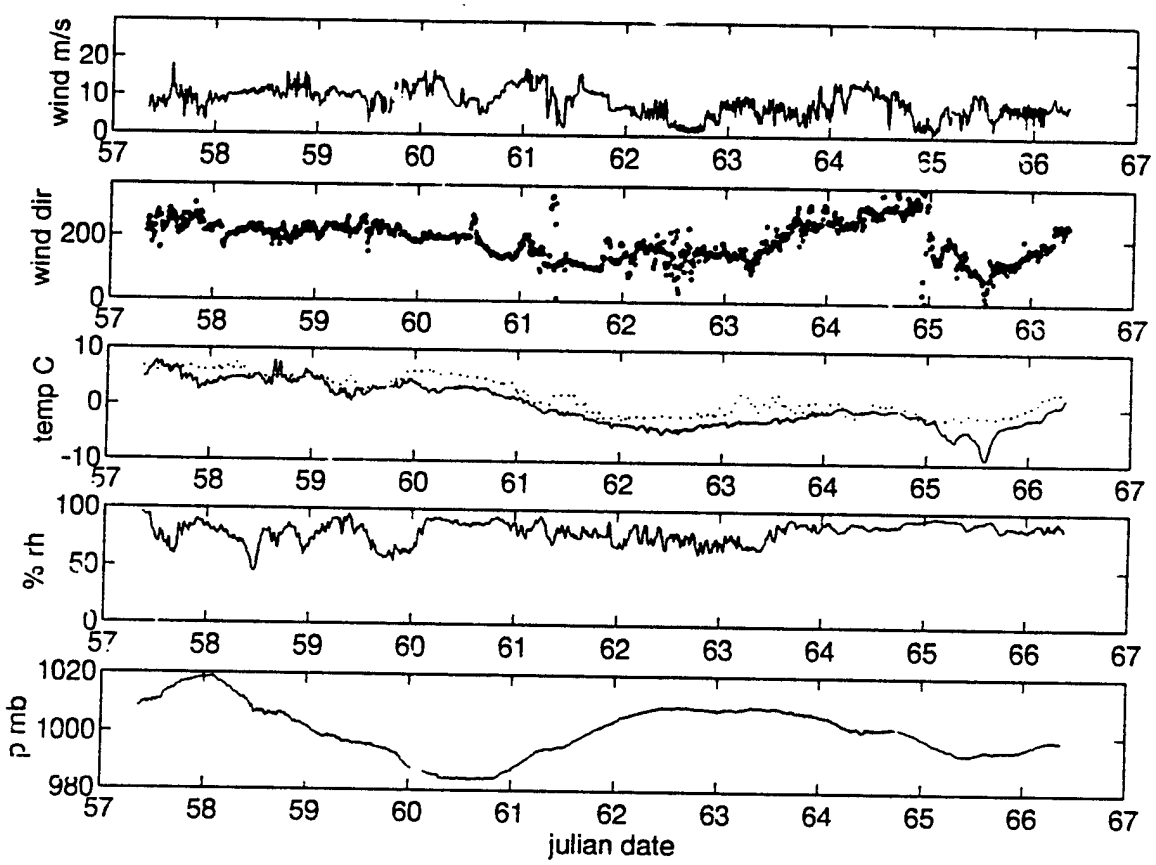

Figure 3.7 Time series of wind speed, wind direction, sea surface temperature (dotted) and air temperature (solid), relative humidity and pressure during SIZEX in the Barents Sea, March 1992.

IV. HEAT FLUX COMPUTATIONS USING THE BULK METHOD

A. THEORY

The primary goal of this thesis is to quantify the turbulent heat flux between the ocean and atmosphere in the Greenland, Norwegian and Barents Sea regions. This goal is accomplished through use of the bulk aerodynamic method which is based on Monin-Obukhov (M-O) similarity theory.

The bulk method has proven to be an accurate method for computing heat fluxes between the ocean and atmosphere (Blanc, 1985). This method is the most practical for shipboard-based measurements, requiring only routine meteorological measurements such as wind speed, air temperature, sea surface temperature, relative humidity and atmospheric pressure. The bulk method allows calculations to be made based on measurements made from ships at sea, which provide a substantial portion of the data available over the oceans.

Monin-Obukhov similarity theory assumes the gradients of the meteorological variables depend on surface fluxes, height and stability only. For instance, the wind is modeled using the log wind profile modified for stability effects. Therefore, if the wind speed is known at any height within the surface layer, one can estimate the wind speed at any other height within the surface layer (Equation 4.1). Likewise, the profiles of temperature and moisture can be used to estimate sensible and latent heat fluxes. The profiles for temperature and humidity are known and can be found by Equation 4.2,

$$\frac{\partial u}{\partial z} = \frac{u_*}{kz}\phi_M \qquad (4.1)$$

$$\frac{\partial T}{\partial z} = \frac{T_*}{kz}\Phi_T \qquad (4.2)$$

Where u(m/s), T (C) and z(m) are wind speed, potential temperature and observation height; u_* (m/s) is a velocity scale called the friction velocity, T_* (C) is a surface layer temperature scale; k is Von Karman's constant; and Φ_M and Φ_T are dimensionless wind shear and temperature functions of stability (z/L).

B. BULK FORMULA

The turbulent heat fluxes at the surface can be expressed in the form

$$SHF \equiv \rho c_p \overline{w'T'} = -\rho C_p u_* T_* \qquad (4.3)$$

$$LHF \equiv \rho L_v \overline{w'q'} = -\rho L_v u_* q_* \qquad (4.4)$$

where SHF (W/m^2) and LHF (W/m^2) are sensible and latent heat flux, with the sign convention that a positive value indicates a heat flux from the ocean to the atmosphere and a

negative indicates heat flux from the air to the ocean; The variable ρ (kg/m^3) is atmospheric density, based on surface temperature and pressure and calculated using the ideal gas law; C_p (1004 J/kg K) is the specific heat of dry air; L_v (250000 J/kg) is the latent heat of vaporization at 0°C.

The parameter T_* (C) is a temperature scale and q_* (g water/g air) is a humidity scale. The scaling paramters are calculated using the following equations

$$u_* = \frac{uk}{\ln(\frac{z}{z_0}) - \Psi_m} \qquad (4.5)$$

$$T_* = \frac{(T_{10} - T_s)\ k}{\ln(\frac{z}{z_{0t}}) - \Psi_t} \qquad (4.6)$$

$$q_* = \frac{(q_{10} - q_s)\ k}{\ln(\frac{z}{z_{0q}}) - \Psi_t} \qquad (4.7)$$

where T_{10} (C) and T_s (C) are potential temperature at 10 m and at the surface; q_{10} (g/kg) and q_s (g/kg) are the mixing ratios at 10 m and at the surface; z_0 is roughness length, which is the sum of Charnock's roughness length and the roughness length for a smooth surface and is defined by Equation 4.8; z_{0t} and z_{0q} are the thermal and moisture

roughness lengths based on a constant heat exchange coefficient (C_{hn} and C_{en}) and defined by Equations 4.9 and 4.10;

$$z_0 = (0.011 u_*^2/9.8) + ((.11) (1.4x10^{-5}) / u_*) \qquad (4.8)$$

$$z_{0t} = 10 \exp \frac{-k^2}{c_{tn} \ln(z/z_0)} \qquad (4.9)$$

$$z_{0q} = 10 \exp \frac{-k^2}{c_{en} \ln(z/z_0)} \qquad 4.10$$

Ψ_m and Ψ_t are the integrated stability functions, for unstable stratification and defined by Equations 4.11 and 4.12.

$$\Psi_m = 2 \ln[(1+x)/2] + \ln[(1+x^2)/2] - 2 \arctan(x) + \pi/2 \qquad (4.11)$$

$$\Psi_t = 2 \ln[(1+x^2)/2] \qquad (4.12)$$

$$x = (1 - 16 z/L)^{.25} \qquad (4.13)$$

and for stable stratification

$$\Psi_m = -5\ z/L \qquad (4.14)$$

$$\Psi_t = -5\ z/L \qquad (4.15)$$

L is the Monin-Obukhov stability length defined by Equation 4.16, and z/L is the stability; T_{v*} is the buoyancy flux scaling parameter determined by Equation 4.17,

$$L = \frac{u_*^2\ T_{vs}}{kgT_{v*}} \qquad (4.16)$$

$$T_{v*} = \frac{(T_v - T_{vs})\ k}{\ln(z/z_0) - \Psi_T} \qquad (4.17)$$

where T_v (C) and T_{vs} (C) are the virtual potential temperature at the measurement height and the surface.

The constants in the Charnock relationship (Equation 4.8) and the integrated stability functions are from Smith (1988).

The advantage of using the bulk method is that the only parameters required are the mean wind speed, the mean air temperature and the mean humidity at one level each in the surface layer, and the mean surface temperature. High frequency or multi-level measurements are not required and

the bulk method is less affected by ship effects than are other flux calculation methods.

For the unstable cases (cold air over warm water) and stable cases (warm air over cold water) Ψ_t is a function of the stability parameter (z/L). The surface layer over open water in the Arctic is typically unstable. Therefore, z/L is negative, and the sensible and latent heat fluxes are enhanced by buoyancy effects. However, if the surface layer is stable, which is rare but does occur, then z/L is positive. Thus, Ψ_t is negative and u_*, T_* and q_* would all be smaller in magnitude; this implies the sensible and latent heat fluxes would also be smaller in magnitude.

C. SOLVING FOR HEAT FLUX BY ITERATION

Determining u_*, T_*, and q_* requires knowledge of L, which in turn is a function of u_*, T_* and q_*. Therefore, an iterative solution method is needed.

The first step in the iterative process is to make an initial guess at L, z_0, and u_*. Then Equations 4.5, 4.6, 4.7, 4.8 and 4.16 are repeatedly solved for u_*, z_0 and L until the solution for u_* converges. However, if the wind speed is zero or the atmosphere is too stable, the solution will not converge. In this case the atmosphere is non-turbulent and u_*, T_*, q_* and z/L are set equal to zero. The Matlab program used in calculating heat fluxes can be found in the Appendix.

D. LIMITATIONS OF THE BULK METHOD

The scheme shown above is one of many bulk transfer coefficient schemes. Each of the different schemes contains different coefficients of drag, heat and humidity and varies

in degree of complexity. Some include stability dependence while others ignore stability or assume a constant stability effect. Additionally, each method has a different range of wind speeds and air sea temperature differences under which the method is considered valid. Smith (1988) listed several limitations to his technique, which are summarized below.

1. High Wind Speed

There are few reliable measurements of wind stress and heat flux above 26 m/s. Thus, application of the method to wind speeds above 26 m/s would be an extrapolation of the lower wind speed data. Fortunately, winds above the 26 m/s threshold are absent in all but the SIZEX data set and are rare there.

2. Extremely Stable Stratification

If the atmosphere is too stable then the iterative method will fail to produce a convergent solution. Here the program will give a value of zero for u*, T*, q* and z/L. This implies the fluxes are zero and actual values will be very close to zero. These highly stable conditions would occur if the air temperature was very warm and the sea surface very cold, but such occurrences are rare.

3. Extremely Unstable Stratification

If the wind speed were close to zero then the iterative method would fail to produce a convergent solution. In this case the program will give a value of zero for u*, which implies the fluxes are zero. In fact, there may be fluxes due to convection. Free convective scaling was not included in the bulk formula, but this was judged to not degrade the results since calm conditions and non-convergent solutions are very rare or nonexistent in the data.

V. RESULTS AND COMPARISONS

A. RESULTS OF HEAT FLUX COMPUTATIONS

Turbulent heat fluxes were computed based on the data presented in Chapter III and the method discussed in Chapter IV. Overall, the average measured turbulent heat fluxes (THF) in this thesis (Table 5.1) compared favorably with those given by the climatological studies mentioned previously.

Exercise Date Region	LHF	SHF	THF
CEAREX Mar 89 Greenland Sea	109	140	249
SIZEX Jan 92 Greenland Sea	111	105	216
NORCSEX Mar 88 Norwegian Sea	87	44	131
NORCSEX Nov 91 Norwegian Sea	96	30	126
CEAREX Feb 89 Barents Sea	73	45	118
SIZEX Mar 92 Barents Sea	44	20	64

Table 5.1 Mean value of latent, sensible and total turbulent heat flux (W/m^2).

Heat flux computations for all the NPS ship cruises occurred during the Arctic winter (November - March). Analysis of the climatological data of Bunker (1976) and Gorshkov (1988), showed peak heat loss (positive or upward heat flux) for this region in December and January with only slightly less heat loss in the preceding and following months. Therefore, the time difference in the observations does not significantly hinder comparisons between exercises that occurred in different winter months, and the differences in heat flux values displayed in Table 5.1 are primarily due to the differenecs in the ship's location or differences between years.

According to the data, the largest mean THF, near 250 W/m^2, was seen in the Greenland Sea. The Norwegian Sea had a mean THF of 130 W/m^2, whereas the Barents Sea had the lowest mean THF.

B. COMPARISON WITH PREVIOUS STUDIES

In this section, the calculations of heat flux based on the NPS data are compared with previously published values. Accepted faults with comparisons include: (1) Slightly differing spatial regimes: the mean value of the total turbulent heat flux measurement is taken along a ship track, whereas in the climatological studies locations are fixed or averaged over large areas and HC used grid point data. (2) Different time scales: record length was two to three weeks, whereas the climatological studies have tens of years of data, and HC data comes entirely from one year (1979). However, the bulk method used here, is similar to Bunkers' method, and is considered more advanced than some earlier methods. For example, the method used in this thesis

includes flux computations that account for variable stability (z/L), roughness (z_0) and atmospheric density (ρ).

In the following subsections, the results of each exercise's heat flux computations are reviewed and compared, by region, to the results of the earlier studies.

1. Greenland Sea

During SIZEX, the mean LHF was 111 W/m^2 and the mean SHF was 105 W/m^2. This exercise had some of the largest 10 minute averaged heat fluxes of all the cases (Figure 5.1). These large heat fluxes are a result of the stronger winds and strong to moderate air sea temperature differences (ASTD) encountered in the Greenland Sea during SIZEX. Histograms of THF for all exercises were plotted with 50 equally spaced bins between the maximum and minimum values of THF for that exercise. The histogram for this case (Figure 5.2) showed a maximum occurrence near the median of 210 W/m^2 and a long tail to the right (above 400 $W/m^{2)}$ corresponding to a high wind event on Julian day 14. A false local maximum occurring at 100 W/m^2 is the result of a data gap of about six hours on Julian day 13.

During CEAREX, the heat fluxes (Figure 5.3) were also relatively large compared with other NPS exercises. The mean LHF was 109 W/m^2 and the mean SHF was 140 W/m^2. As in SIZEX, the large heat fluxes can be attributed to large ASTD, large moisture gradients and moderate winds. The large ASTD values are a result of the cold air advection off the ice (northerly winds). Mean winds (9.1 m/s) for the Greenland Sea region during CEAREX are similar to other exercises and had a small standard deviation (2.7 m/s) compared with other exercises. Nevertheless, the heat fluxes are larger in the Greenland Sea primarily due to the colder air over the Greenland Sea. The histogram of the

heat flux (Figure 5.4) has at least three peaks. The different peaks are the result of changes in synoptic conditions. The largest number of occurrences is at 330 W/m^2 and is related to the cold air outbreak on Julian days 71 through 75. During this period the highest heat fluxes were caused by cold air advection, and occurred after the winds backed to the north and result in a highly unstable surface layer (very cold air over warmer water). The second peak is near 200 W/m^2 and is the result of smaller winds and ASTD after Julian day 75. The third local maximum at 60 W/m^2, occurred during a pressure minimum, and was the result of the southerly winds that gave an unstable surface layer (cold air over warmer water).

The VT heat flux data compared well with the January SIZEX data, but were 20% larger than the March CEAREX observations of heat flux (Tables 5.2 and 5.3). The Gorshkov data showed mixed results. Their values for heat flux during SIZEX were within 10% and during CEAREX were 70% less than computed for the NPS data set. The HC heat fluxes were two to three times larger than any other computed heat flux during January, and were 20% larger than the NPS values during CEAREX, which was in March.

Exercise	LHF	SHF	THF
SIZEX GS	111	105	216
VT	59	142	201
Gorshkov	126	116	242
HC	NA	NA	640

Table 5.2 Latent, sensible and total turbulent heat flux (W/m^2) over the Greenland Sea in January.

Exercise	LHF	SHF	THF
CEAREX GS	109	140	249
VT	89	206	295
Gorshkov	73	73	146
HC	NA	NA	300

Table 5.3 Latent, sensible and total turbulent heat flux (W/m^2) over the Greenland Sea in March.

2. Norwegian Sea

NORCSEX 88 was conducted in March 1988, off the southwest coast of Norway. Heat fluxes for this exercise were similar to previous results for the area (Table 5.4). The mean LHF was 87 W/m^2 and the mean SHF was 44 W/m^2.

The heat flux (Figure 5.5) exhibits a synoptic influence, which should be expected in a stormy region of the Norwegian Sea. For example, before the passage of a

series of surface cyclones on Julian day 71 the THF is small (50 W/m^2) due to low winds and a small ASTD. Afterwards, the wind speed and ASTD increased causing the THF to climb above 200 W/m^2 and then decreased to around the mean of 130 W/m^2 after the winds died down. Also, the SHF time series is strikingly similar to the time series of wind speed (as seen in Chapter III, Figure 3.1). The histogram of heat flux (Figure 5.6) is nearly symmetric with a sharp peak near the median of 120 W/m^2. The tail of fluxes above 250 W/m^2 represents a mesoscale gale force storm observed for several hours on Julian day 71.

NORCSEX 91 was conducted in the southern Norwegian Sea in November 1991. The THF values for this exercise (Figure 5.7) were similiar to those of NORCSEX 88. During NORCSEX 91, the SHF was low with a mean 30 W/m^2. The LHF was larger, with a mean value of 96 W/m^2. NORCSEX 91 experienced the passage of several cyclones with associated wind variations. The heat fluxes modulated with these wind changes. Also, apparent is the effect of the ASTD. During the earlier periods with larger ASTD the fluxes are larger but after Julian day 328 when the ASTD became smaller the flux decreased. The histogram of THF (Figure 5.8) has three modes. The first mode, near 0 W/m^2, was a result of the small or zero ASTD that occurred from Julian day 333 to 335. Modes two and three occurring at 90 W/m^2 and 170 W/m^2 are the result of a bimodal distribution about the median of 125 W/m^2.

The differing data sets compare well within this region as all the data sets are within 20% - 30% of the mean observed THF (Tables 5.4 and 5.5).

Exercise	LHF	SHF	THF
NORCSEX 88	87	44	131
VT	95	54	149
Gorshkov	97	65	162
HC	NA	NA	100

Table 5.4 Latent, sensible and total turbulent heat flux (W/m^2) over the Norwegian Sea in March.

Exercise	LHF	SHF	THF
NORCSEX 91	96	30	126
VT	67	32	99
Gorshkov	89	61	150
HC	NA	NA	160

Table 5.5 Latent, sensible and total turbulent heat flux (W/m^2) over the Norwegian Sea in November.

3. Barents Sea

A segment of CEAREX was conducted in the Barents Sea in February and early-March 1989. During CEAREX in the Barents Sea the mean LHF was 73 W/m^2 and the mean SHF was 45 W/m^2. Several cyclones seen in the data are apparent in the time series of heat flux as peaks at intervals of two to three days (Figure 5.9). The histogram of THF (Figure 5.10) is skewed to the right and has some high peaks at 80 W/m^2.

Also noticeable are the negative fluxes (heat flux into the ocean) resulting from the surge of warm southerly air and stable conditions around Julian day 66.

SIZEX was conducted in the Barents Sea in March. The THF values for March in the Barents Sea were small, near 60 W/m^2. During SIZEX, the LHF was 44 W/m^2 and the SHF was 20 W/m^2. The heat fluxes are smaller here due to smaller ASTD (Figure 5.11). The histogram of THF (Figure 5.12) is symmetric with a median of near 60 W/m^2.

The heat fluxes of VT and Bunker are up to two times greater than observed by NPS ship data in the Barents Sea (Tables 5.6 and 5.7). However, the Gorshkov and HC heat fluxes are three to four times larger than the measured values. The values of heat flux in the NPS data are strongly influenced by the lack of SST data and the assumption of a constant 1.8 C SST for CEAREX. For example, if the average values for all other directly measured quantities (wind speed, air temp, rh, p) were unchanged and the average SST was assumed to be 0 C vice 1.8 C, the THF would become 60 W/m^2, nearly half. If the average SST were 5 C, the THF would become 230 W/m^2 or nearly double the estimated value. Normally SST would not be so important. However in this instance it is critical because the assumed SST (1.8 C) and the actual mean air temps (-1.4 C) are similar.

Exercise	LHF	SHF	THF
CEAREXBS	73	45	118
VT	64	60	124
Gorshkov	112	161	273
Bunker	100	90	190
HC	NA	NA	400

Table 5.6 Latent, sensible and total turbulent heat flux (W/m^2) over the Barents Sea in February.

Exercise	LHF	SHF	THF
SIZEX BS	44	20	64
VT	90	86	176
Gorshkov	100	145	245
Bunker	100	80	180
HC	NA	NA	240

Table 5.7 Latent, sensible and total turbulent heat flux (W/m^2) over the Barents Sea in March.

C. LIMITATIONS OF PREVIOUS STUDIES

1. Time Averaging Methods

Hanawa and Toba (1987) (hereafter HT) made comparisons of data averaged over various time periods from one day to a month using the sampling method (SM) and the scalar averaging method (SAM). The sampling method (SM) is a simple average of fluxes computed from hourly (or every observation) values of the bulk meteorological parameters (wind, temperature and humidity). The scalar averaging method computes the average flux from average values of the bulk data, thus ignoring correlations between variables. Both methods were compared with data taken every three hours from a mid-latitude Oceanographic Weather Station (OWS-T) (29N 135E) from June 1950 to November 1953. HT showed that the SHF was almost the same regardless of method and averaging time. Also, LHF values computed by the SAM are about 105% of those by the SM for averaging times from three days to one month.

Ledvina et al. (1993) made comparisons similar to HT, using averaging times from 2-72 hours. Their ratios vary little for times exceeding 36 hours, thereby eliminating the need to extend the averaging period beyond 72 hours. Their data was in the equatorial Pacific near 000N 145E from 17 February to 10 March 1990. Like HT, they showed the SAM overestimated LHF with increasing averaging period. Yet with results drastically different from HT, they showed the SAM to underestimate SHF by 40%. Much of this difference may be related to convection in the tropics, thereby demonstrating the importance of regional influences on heat fluxes.

The purpose of this subsection is to extend the work completed by HT and Ledvina et al. (1993) to the polar

latitudes with recent data, thus providing a basis for determining the accuracy of heat fluxes computed via various averaging techniques in the polar seas. Ideally, time averages are desired that are long enough to include all low frequency effects (synoptic) and sampled fast enough to capture all high frequency effects (Kaimal and Finnigan, 1994).

Esbensen and Reynolds (1981) define the sampling method for calculating SHF and LHF in the following equations

$$\overline{SHF} = \rho c_p \overline{C_H U \Delta T} \quad (5.1)$$

$$\overline{LHF} = \rho L_v \overline{C_E U \Delta q} \quad (5.2)$$

where averaging is indicated by the overbar. The key feature of this method is that heat fluxes are calculated for every measurement. The measurement interval was 10 minutes in the NPS data set, generally 3 hours in Bunker's data to 12 hours in the HC model. The fluxes are then summed and then averaged.

The scalar averaging method (classical method) for computing heat flux defines the flux in the following forms

$$\overline{SHF} = \rho C_p \overline{C_H}\, \overline{U}\, \overline{\Delta T} \quad (5.3)$$

$$\overline{LHF} = \rho L_v \overline{C_E}\, \overline{U}\, \overline{\Delta q} \quad (5.4)$$

where the average transfer coefficients of heat and humidity are computed empirically from the sample means of temperature difference, humidity difference and wind speed. The difference of the classical method (SAM) from the sampling method is the measurements are averaged, usually over the entire month and then the heat fluxes are computed based on the averages of the measurements.

Lumley and Panofsky (1964) suggest that a reasonable averaging time for average mean horizontal winds (and temperature) would be 30 minutes, corresponding to the passage of two to three large convective cells through the depth of the convective boundary layer. However, if averaging periods are increased to about one hour, nonstationarity in the form of diurnal variations will occur. With averaging periods of one hour or greater, errors of 5% and 10-50% for T_* and u_* result.

Bunker (1976) and HC used the sampling method when calculating their heat fluxes; VT and Gorshkov (1988) used the classical approach or scalar averaging method. Finally, data from this study are used to compare the sampling method with the classical method in the Greenland, Norwegian and Barents Seas.

The approach of Bunker (1976) was to include every ship or buoy report and compute heat fluxes and then average the fluxes over the month. This method was better than the classical approach in that it would not result in errors due to diurnal fluctuations. The classical approach used by Gorshkov (1988) and VT also has it advantages. Since the covariance and correlation of $U\Delta T$ and $U\Delta q$ are small at shorter time intervals and increase for longer periods, the classical method may provide a better heat flux estimate when the data set is small (Ebsensen and Reynolds, 1981). The smaller covariance at shorter time periods probably

comes from the fact that stronger winds cause more mixing and thus decrease ΔT and Δq.

Results from NPS cruise data show the SAM (using average wind speeds, temperatures, relative humidities and pressures for the entire period of the exercise) gave heat flux results that are ~5% (6% LHF and 3% SHF) larger than when using the sampling method (Table 5.8).

Exercise Region	LHF	SHF	THF
CEAREX Greenland Sea	1.095	1.000	1.037
SIZEX Greenland Sea	1.054	1.071	1.062
NORCSEX 88 Norwegian Sea	1.052	1.077	1.062
NORCSEX 91 Norwegian Sea	1.068	0.997	1.055
CEAREX Barents Sea	1.130	0.990	1.086
SIZEX Barents Sea	0.941	1.005	0.961

Table 5.8. Ratio of heat flux (W/m^2) calculated using time averages of meteorological variables versus using the sampling method.

2. Stability Dependence

If stability is neglected, then one must assume neutral or near neutral conditions and buoyant convection would be negligible. However, neutral stability is rare and unstable conditions prevailed during the NPS exercises. The effect of stability is applied through use of the stability functions (Ψ_m and Ψ_t) defined in Equations 4.11 and 4.12 for unstable stratification and Equations 4.14 and 4.15 for stable stratification. For unstable stratifications (negative z/L) both stability functions (Ψ) are complex functions of stability, and their values will be relatively small and negative thus yielding larger LHF and SHF than under neutral conditions. For stable stratification (positive z/L), Ψ is a linear function of stability (Ψ = -5z/L) and will always yield smaller LHF and SHF than neutral conditions.

The method used by Bunker accounts for stability. HC however, do not explicitly include stability in their calculations.

3. Transfer Exchange Coefficients

The average C_e and C_h for the NPS Barents Sea exercises were 1.35×10^{-3} and 1.13×10^{-3}, respectively. If Bunker's nomogram for transfer coefficients were used instead, that value would be 1.58×10^{-3}. This 17% and 40% increase in the exchange coefficients would lead to a corresponding increase in LHF and SHF. Bunker's C_{en} and C_{hn} values for near-neutral conditions were strongly dependent upon wind speed and ΔT. This dependence on wind speed is however unwarranted as there does not seem to be conclusive experimental evidence for variation of C_e and C_h with wind speed (Smith, 1988).

HC heat flux errors would result from the use of constant exchange coefficients, vice coefficients that vary

with wind speed, temperature gradient, humidity gradient and stability. HC fixed C_e and C_h at $1.5x10^{-3}$ for all regions. In contrast, the coefficients used here varied by region with C_h having a range of $1.0x10^{-3}$ to $1.25x10^{-3}$ with an average of $1.13x10^{-3}$ and C_e having a range of $1.2x10^{-3}$ to $1.5x10^{-3}$ with an average of $1.35x10^{-3}$. If calculating fluxes for our exercises, this variation would cause HC to overestimate SHF nearly 45% in the Barents Sea and 27% in the Norwegian and Greenland Seas and to overestimate LHF 25% in the Barents Sea and 9% in the Norwegian and Greenland Seas.

4. Other Factors

As discussed in Chapter II, the VT data are divided into five degree latitudinal sections and no distinctions are made for longitude. Based on this I have labeled the VT 75N - 80N region as the Greenland Sea, their 75N - 70N as the Barents Sea and their 70N - 65N as the Norwegian Sea. These distinctions are not absolutely accurate in a geographic sense, but they are fitting with the climatological stations of Gorshkov and Bunker and with our ship cruise data.

Haikkinen and Cavalieri used gridded data for the calculation of heat flux. Thus, comparison of locations should be easily accomplished. However, their data was for only one year (1979), which will likely cause errors when comparing with different years. Other errors might occur by use of model data vice observed. If the model was biased toward higher winds or colder air temperatures then larger heat fluxes would be shown. Additionally, the coarse model grid (250km) does not have the resolution to accurately portray the large horizontal gradients of temperature and wind speed that occurs at the ice edge (Personal

communication Guest, 1995). This may in part account for their large flux gradients near the ice edge.

D. POWER SPECTRAL DENSITY OF HEAT FLUXES

Power spectral densities (psd) of heat flux for all exercises were also examined. The power spectral density function estimates the signal of heat flux as a function of frequency. Windowing was performed using a Hanning window. The sampling frequency that varied for each exercise based on the record length was used for scaling plots. One half of the sampling frequency (1 / 600 sec) would be the highest resolvable frequency (Nyquist frequency). The lowest resolvable frequency would be 1 / the total time of each exercise.

All the power spectral density plots (Figures 5.13 - 5.18) exhibited a peak in power between $1x10^{-5}$ - $5x10^{-6}$ Hz, corresponding to 1-2 days. This illustrates that most of the power is at the synoptic period. The typical slope of the psd function at the higher frequencies (above 10^{-5} Hz) corresponding to periods less than one day was -1.5 in log-log space.

E. ACCURACY OF HEAT FLUX MEASUREMENTS

The largest source of uncertainty for SHF and LHF measurements is sensor accuracy (Blanc 1987). Using the manufacturers published sensor errors along with field experience (Table 5.9) an error estimate (Tables 5.10 and 5.11) caused by sensor inaccuracies, ship contamination and radiation contamination for our exercises was determined in a root mean square manner (Equations 5.1 and 5.2).

Air temperature Error	1.0 C
Sea temperature Error	1.0 C
ASTD Error	1.4 C
Relative Humidity Error	5%
Abs. Humidity Error at -10 C	0.1 g/Kg
Abs. Humidity Error at 0 C	0.2 g/Kg
Abs. Humidity Error at 10 C	0.4 g/Kg
Wind Speed Error	0.3 m/s

Table 5.9 Possible measurement errors of data used in heat flux calculations.

$$SHF_{err} = \sqrt{(\rho c_p C_h (\Delta T_{err}) (U))^2 + (\rho c_p C_h (\Delta T) (U_{err}))^2} \quad (5.1)$$

$$LHF_{err} = \sqrt{(\rho L_v C_e (\Delta q_{err}) (U))^2 + (\rho L_v C_e (\Delta q) (U_{err}))^2} \quad (5.2)$$

	5 m\s	10 m\s	15 m\s	20 m\s	25 m\s
0 C	10.3	20.6	30.8	41.1	51.4
-5 C	10.5	20.7	30.9	41.2	51.5
-10 C	11.4	21.2	31.2	41.4	51.7
-15 C	12.2	21.6	31.5	41.9	51.8
-20 C	13.5	22.4	32.0	42.0	52.2

Table 5.10 Possible error in sensible heat flux (W/m^2) measurement as a function of wind speed and ASTD.

	5 m\s	10 m\s	15 m\s	20 m\s	25 m\s
0 g\Kg	8.8	17.6	26.3	35.1	43.9
-1 g\Kg	8.9	17.7	26.3	35.1	43.9
-2 g\Kg	9.2	17.8	26.4	35.2	44.0
-3 g\Kg	9.6	18.0	26.6	35.3	44.1

Table 5.11 Possible error in latent heat flux (W/m^2) measurement as a function of wind speed and air-sea humidity diference.

The random SHF and LHF errors for average values of wind speed (10 m/s), ASTD (-5 C) and air-sea humidity difference (-1.5 g/Kg) from the NPS data set would be 21 W/m^2 and 18 W/m^2 respectively. Therefore the random THF

error would be about 27 W/m^2, when added in a root mean square fashion. Random errors can however be reduced by increasing the number of averaging operations done. This can be accomplished without changing method by taking more measurements. Systematic (non-random) errors are also present and cannot be reduced by averaging. The worst case non-random error for the NPS exercises would be 39 W/m^2.

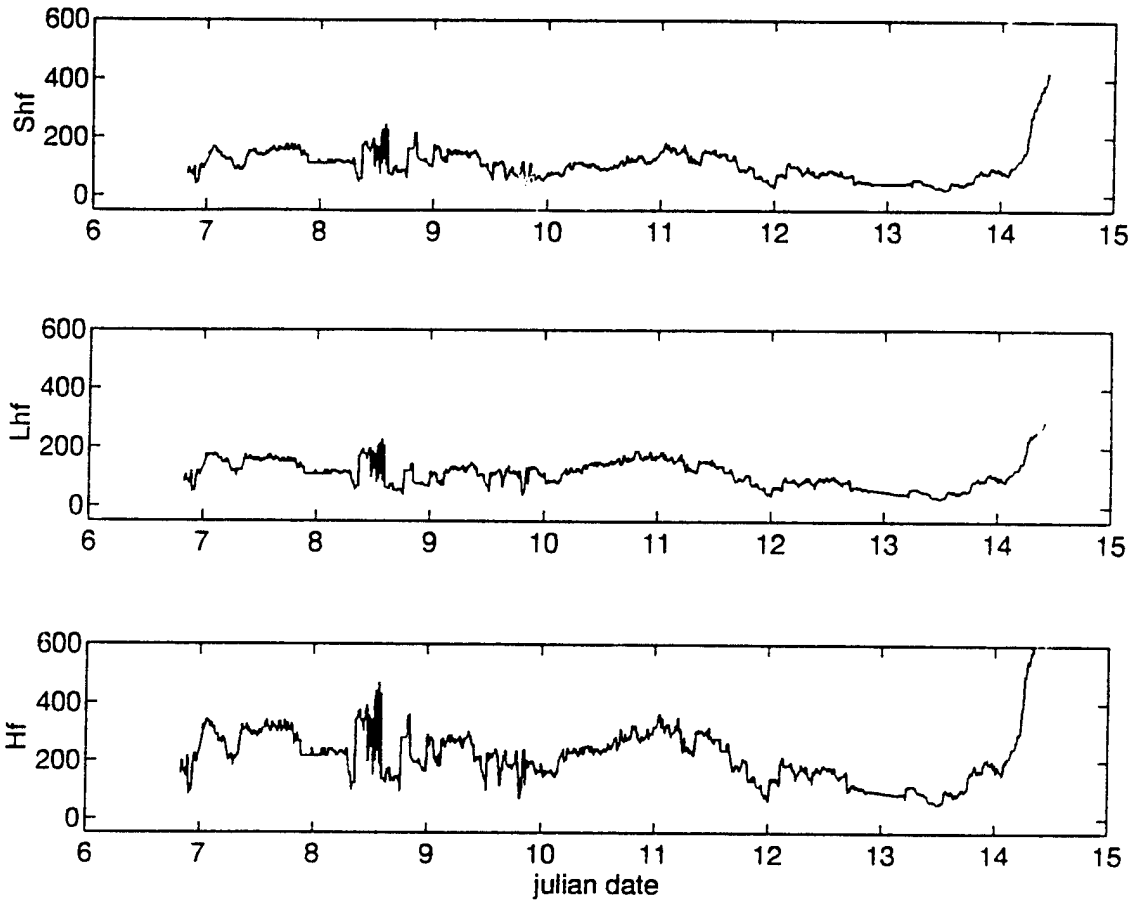

Figure 5.1 Time series of sensible, latent and total turbulent heat flux (W/m^2) for SIZEX in the Greenland Sea, January 1992.

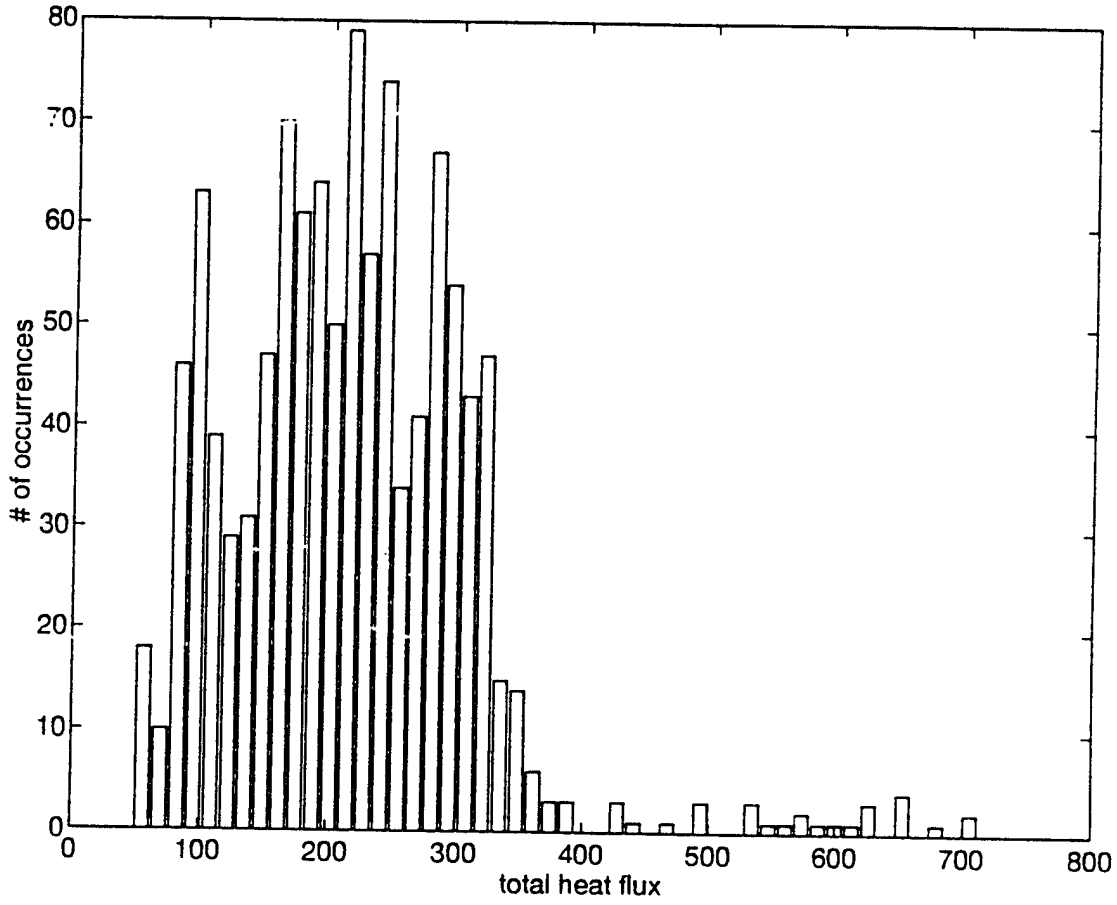

Figure 5.2 Histogram of total turbulent heat flux (W/m^2) for SIZEX in the Greenland Sea, January 1992.

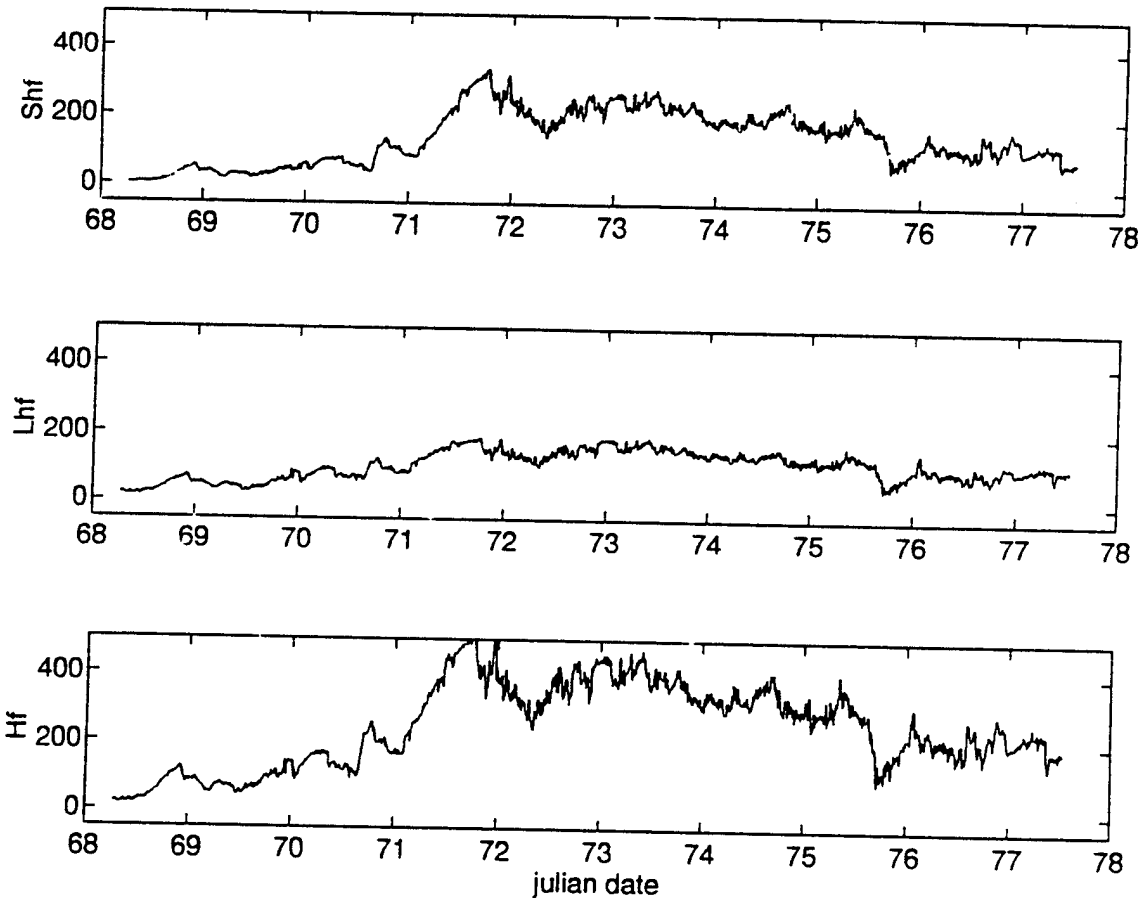

Figure 5.3 Time series of sensible, latent and total turbulent heat flux (W/m^2) for CEAREX in the Greenland Sea, March 1989.

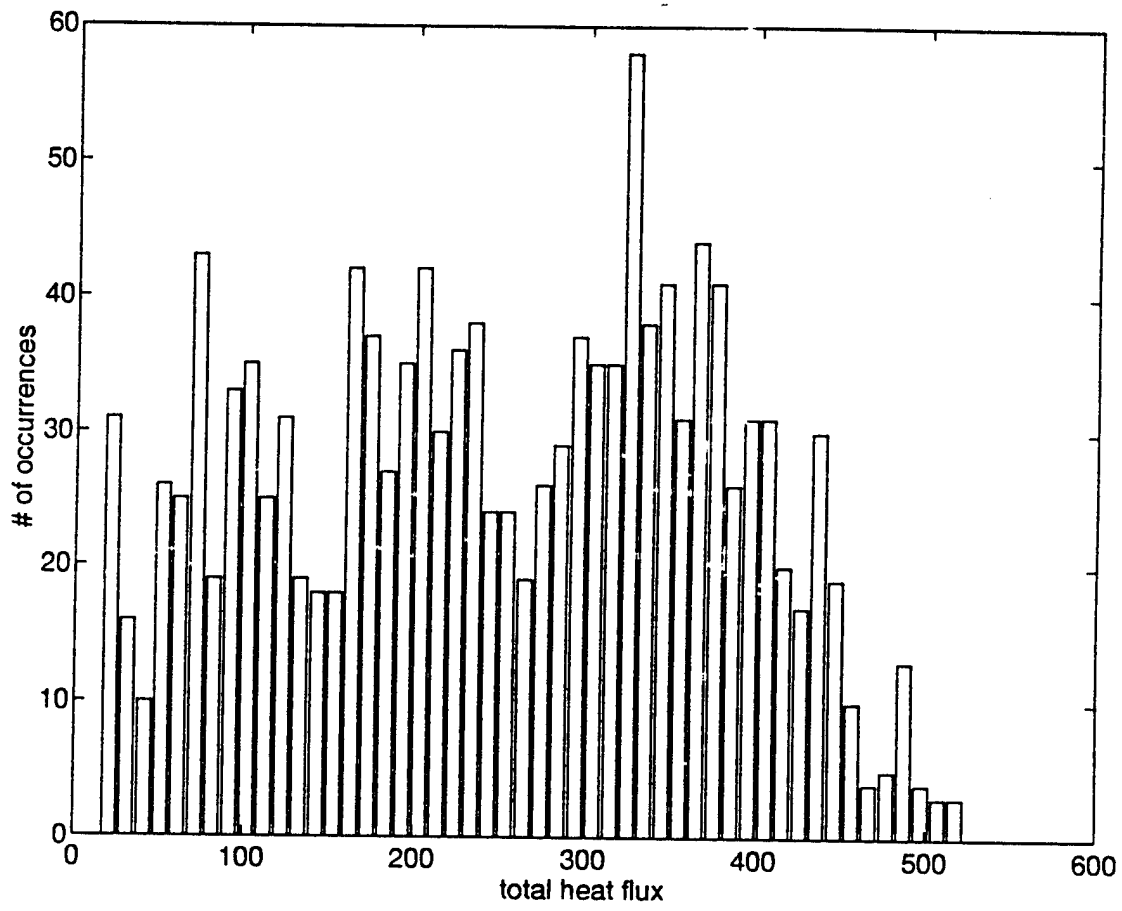

Figure 5.4 Histogram total turbulent heat flux (W/m^2) for CEAREX in the Greenland Sea, March 1989.

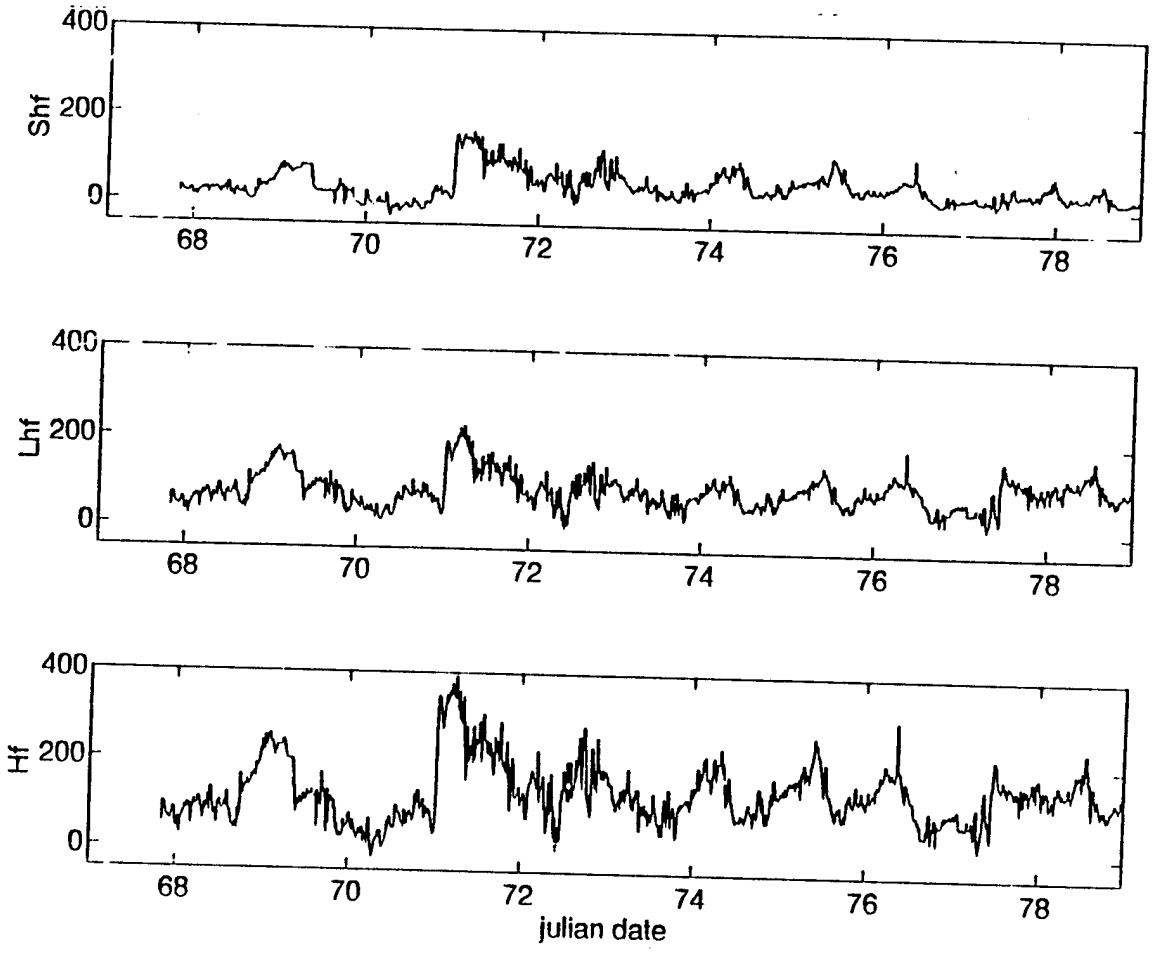

Figure 5.5 Time series of sensible, latent and total turbulent heat flux (W/m^2) for NORCSEX88 in the Norwegian Sea, March 1988.

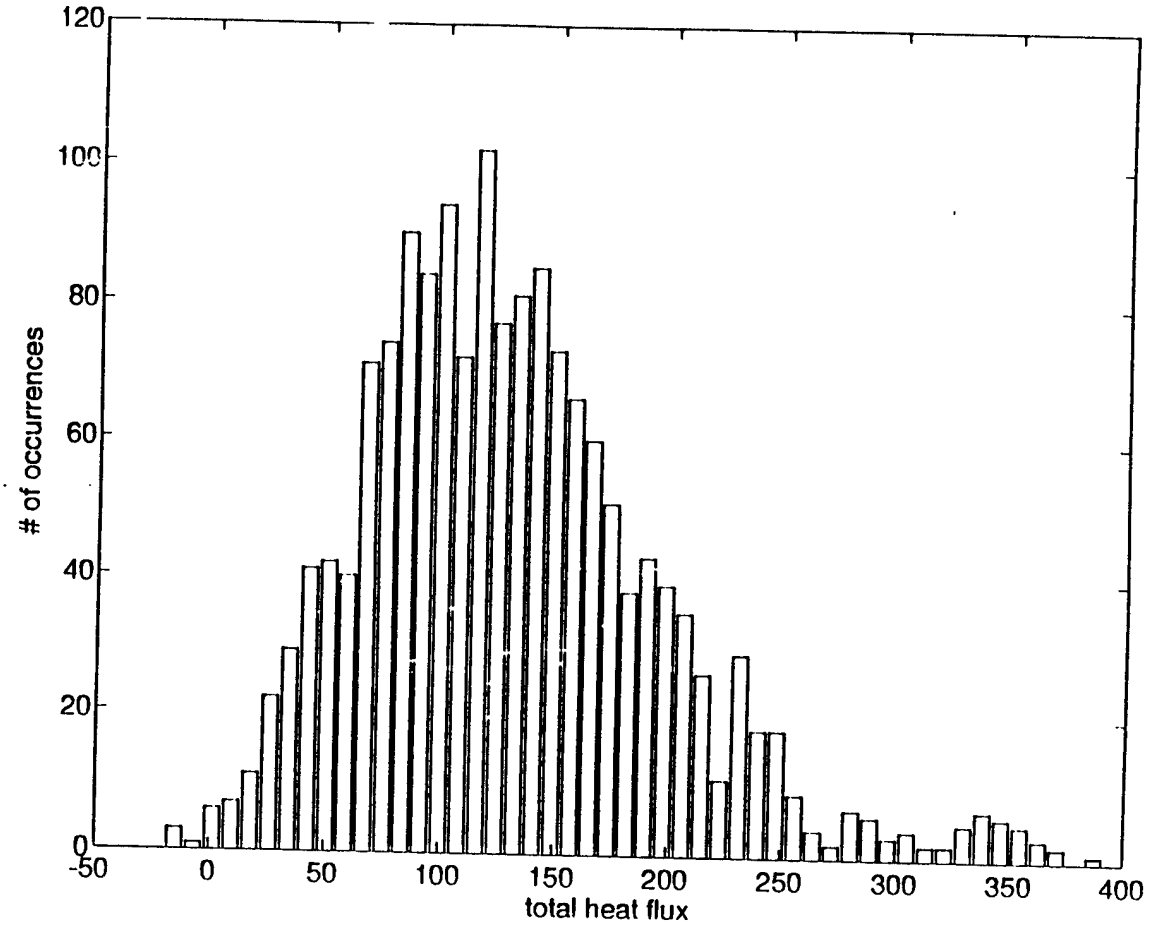

Figure 5.6 Histogram of total turbulent heat flux (W/m^2) for NORCSEX in the Norwegian Sea, March 1988.

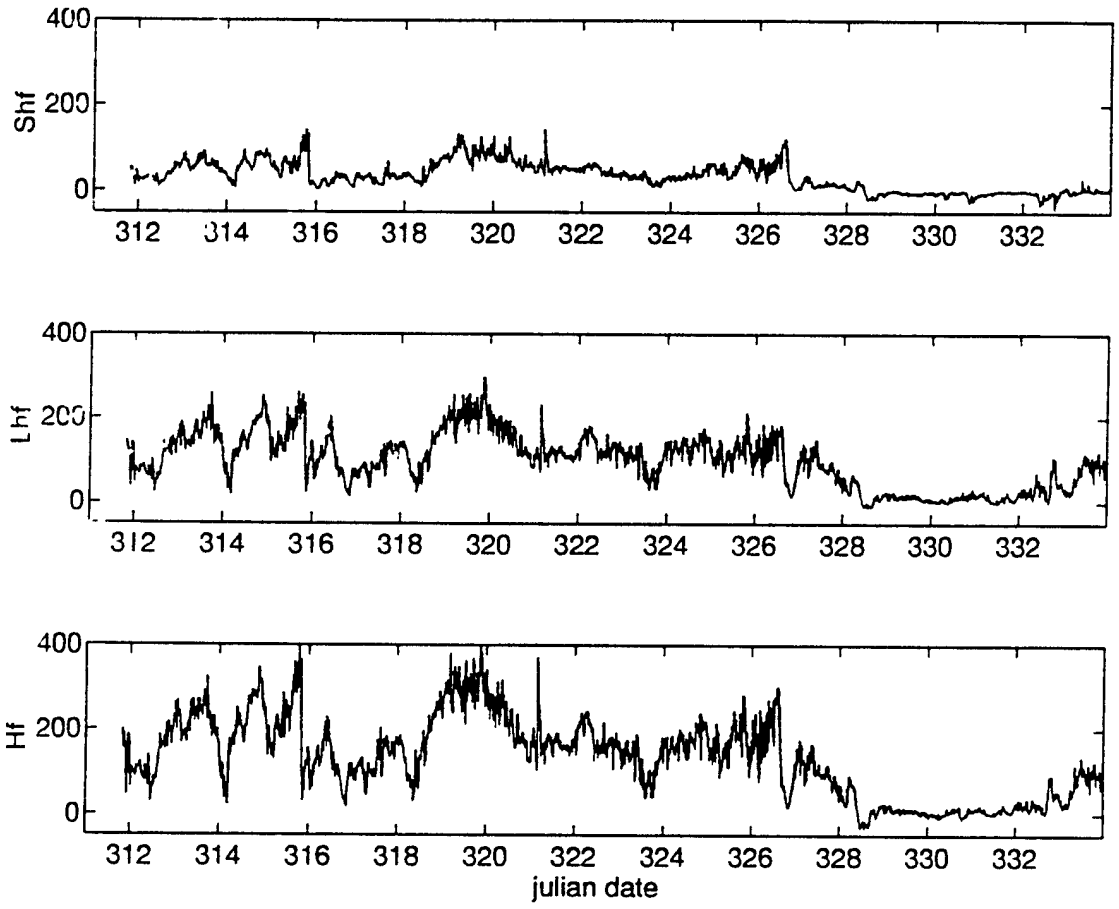

Figure 5.7 Time series of sensible, latent and total turbulent heat flux (W/m^2) for NORCSEX in the Norwegian Sea, November 1991.

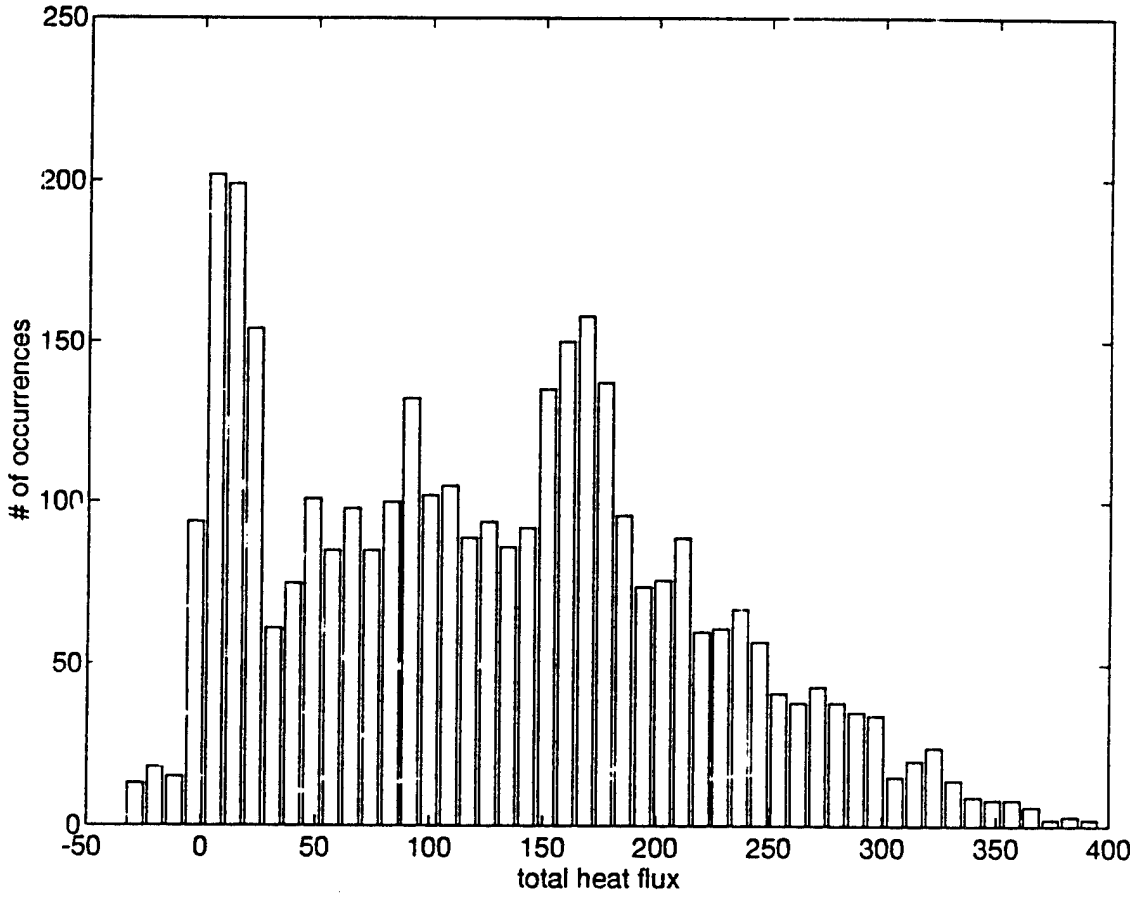

Figure 5.8 Histogram of total turbulent heat flux (W/m^2) for NORCSEX in the Norwegian Sea, November 1991.

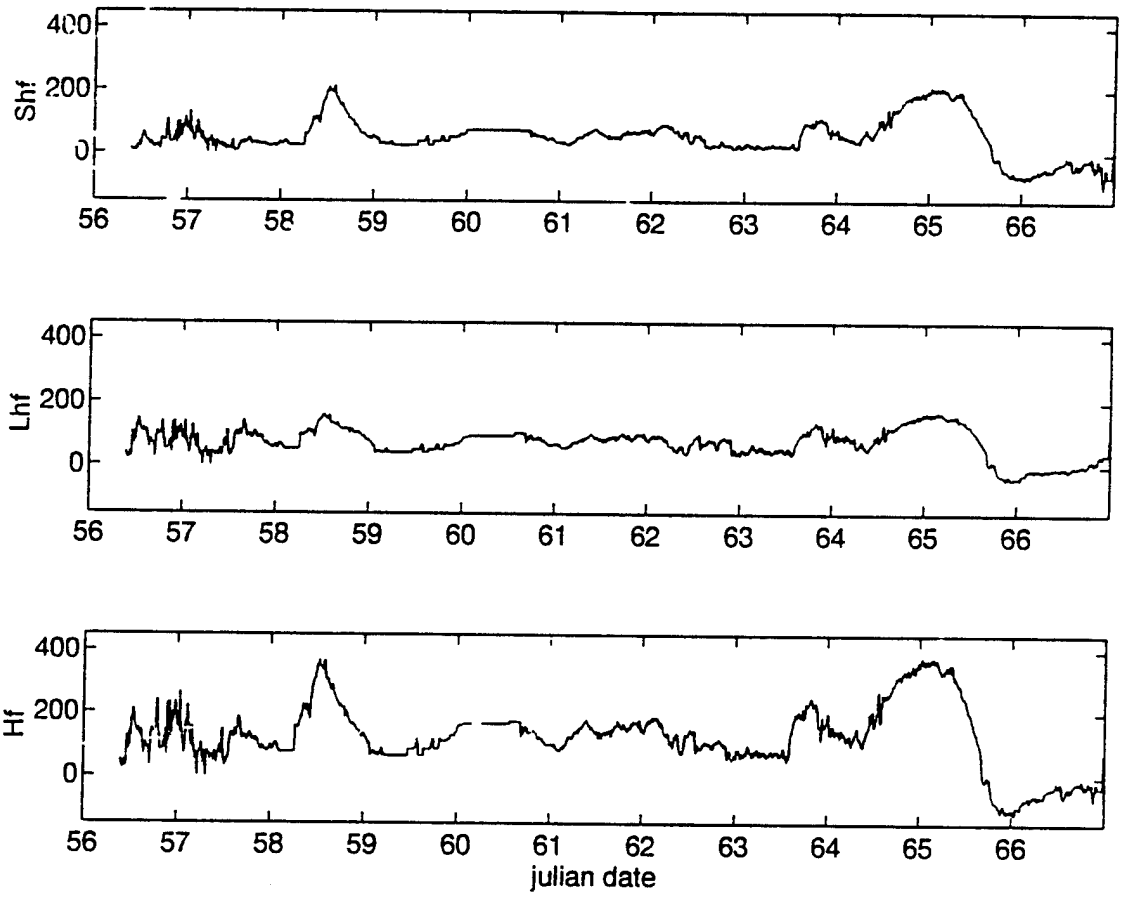

Figure 5.9 Time series of sensible, latent and total turbulent heat flux (W/m^2) for CEAREX in the Barents Sea, February-March 1989.

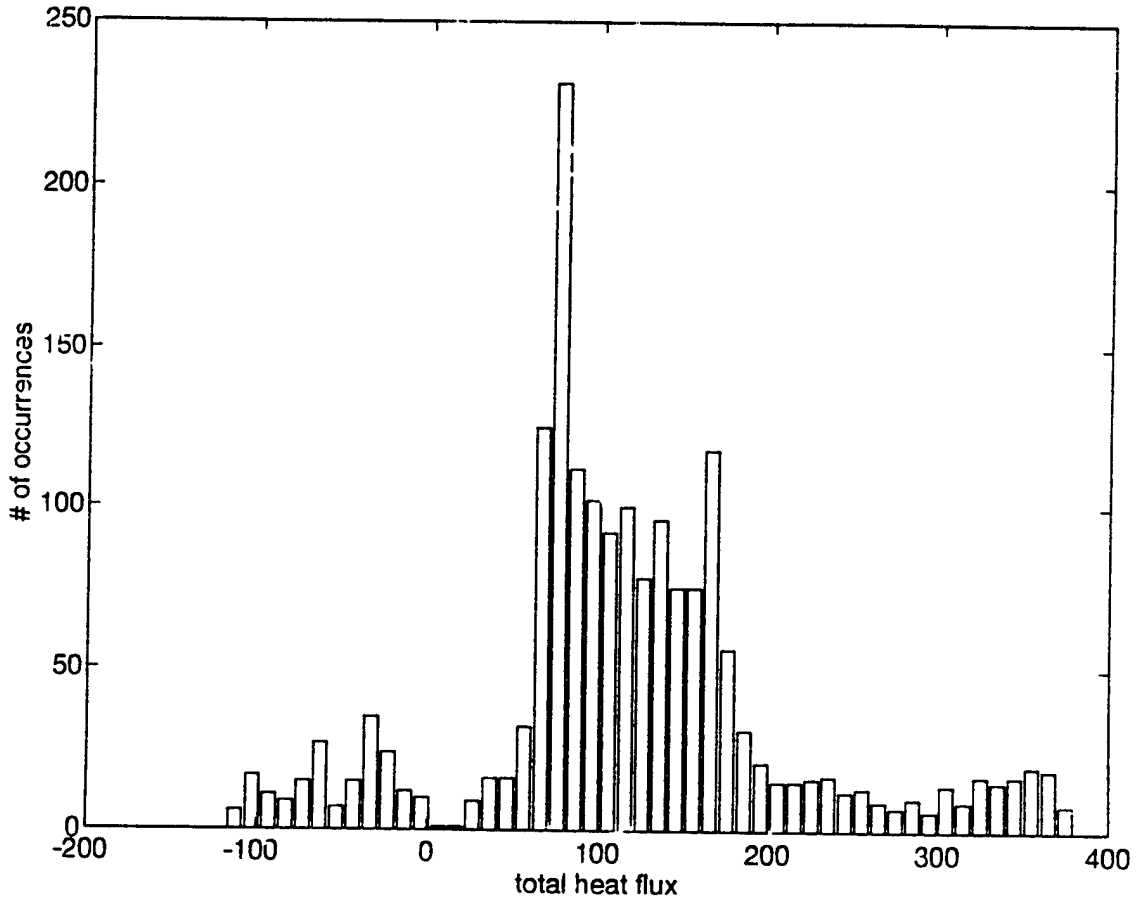

Figure 5.10 Histogram of total turbulent heat flux (W/m^2) for CEAREX in the Barents Sea, March 1989.

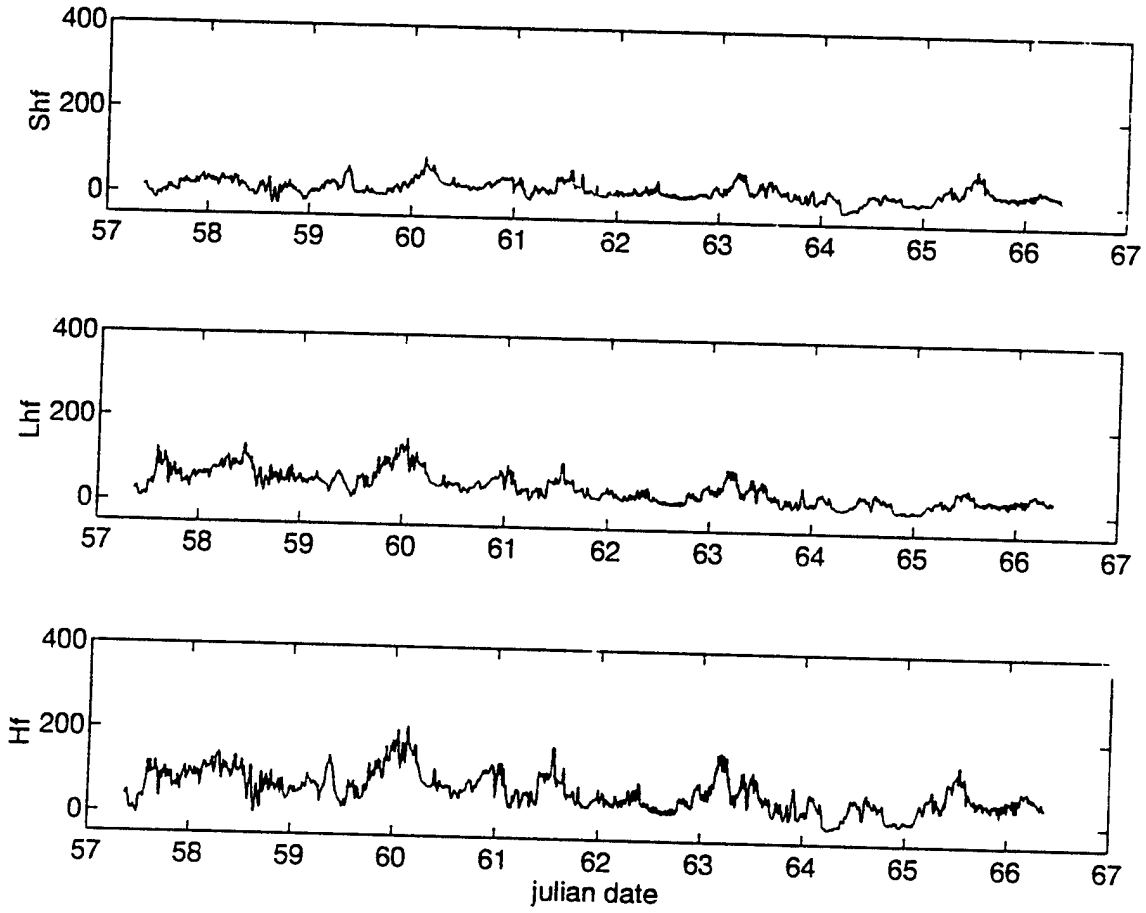

Figure 5.11 Time Series of sensible, latent ant total turbulent heat flux (W/m^2) for SIZEX in the Barents Sea, March 1992.

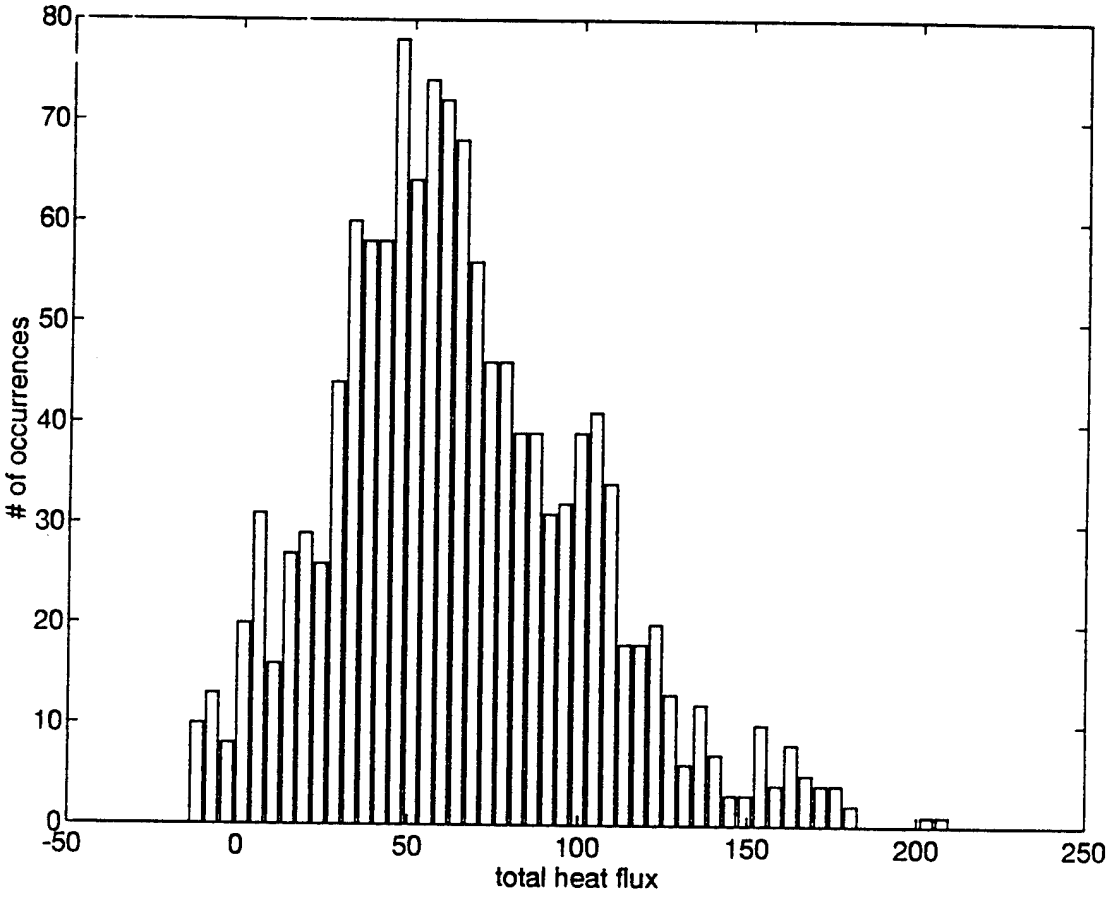

Figure 5.12 Histogram of total turbulent heat flux (W/m^2) for SIZEX in the Barents Sea, March 1992.

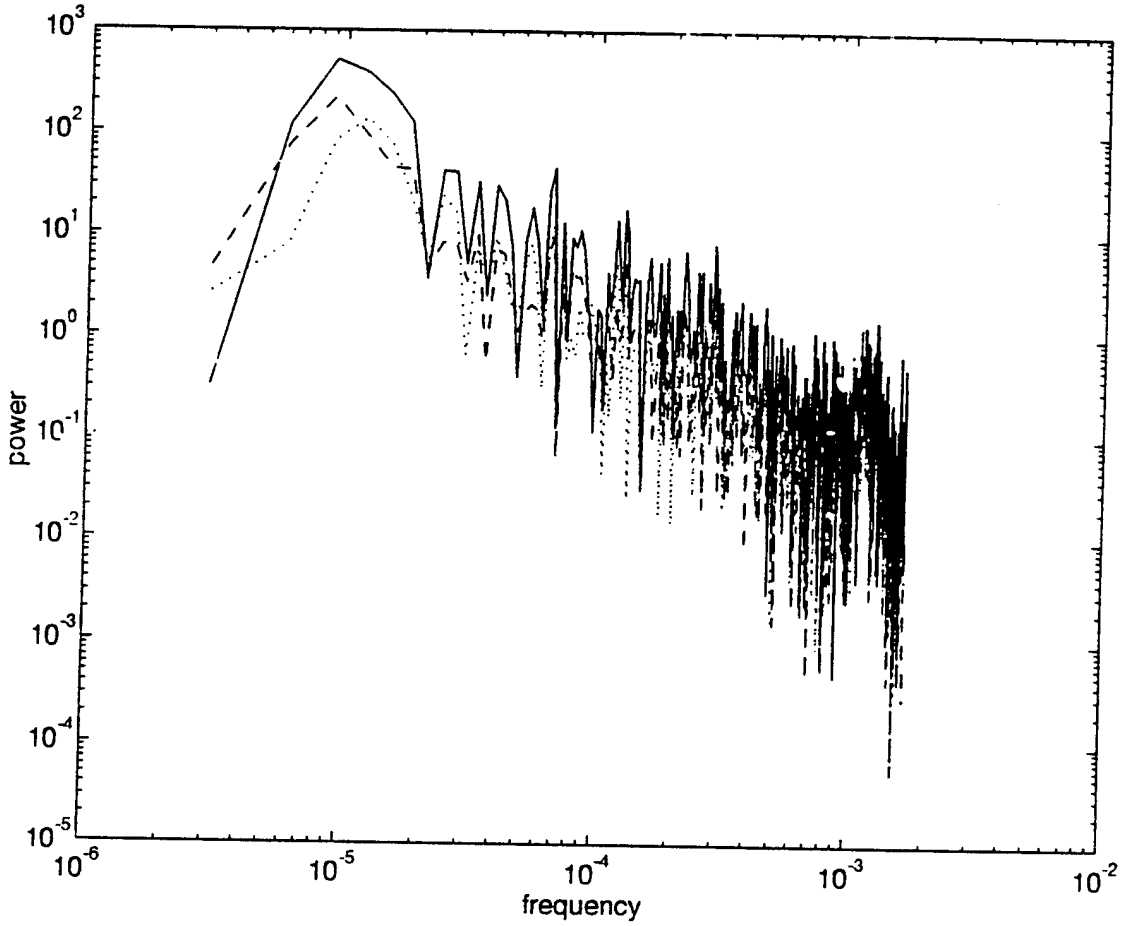

Figure 5.13 Power spectral density of latent (dashed line), sensible (dotted line) and total turbulent (solid line) heat flux (W/m^2) for SIZEX in the Greenland Sea, January 1992.

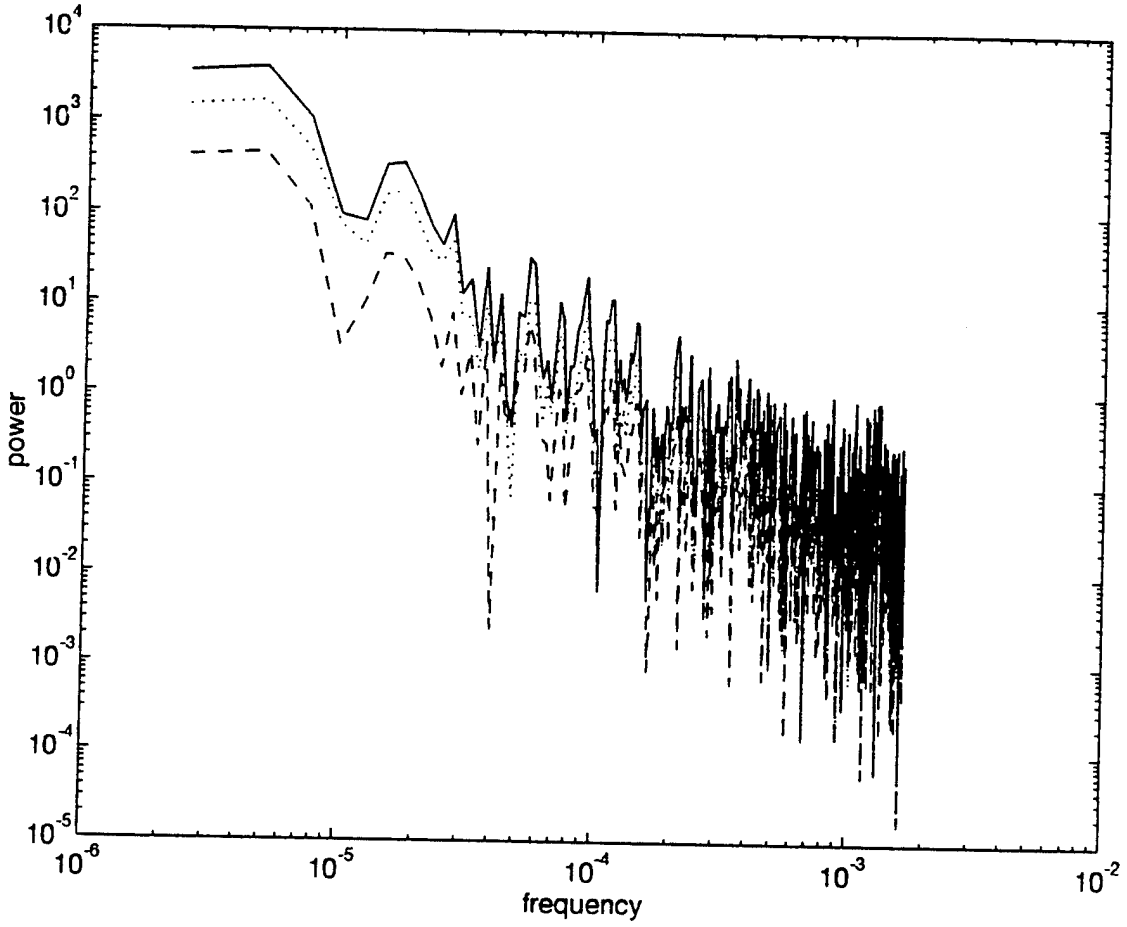

Figure 5.14 Power spectral density sensible (dotted line), latent (dashed line) and total turbulent (solid line) heat flux (W/m^2) for CEAREX in the Greenland Sea, March 1989.

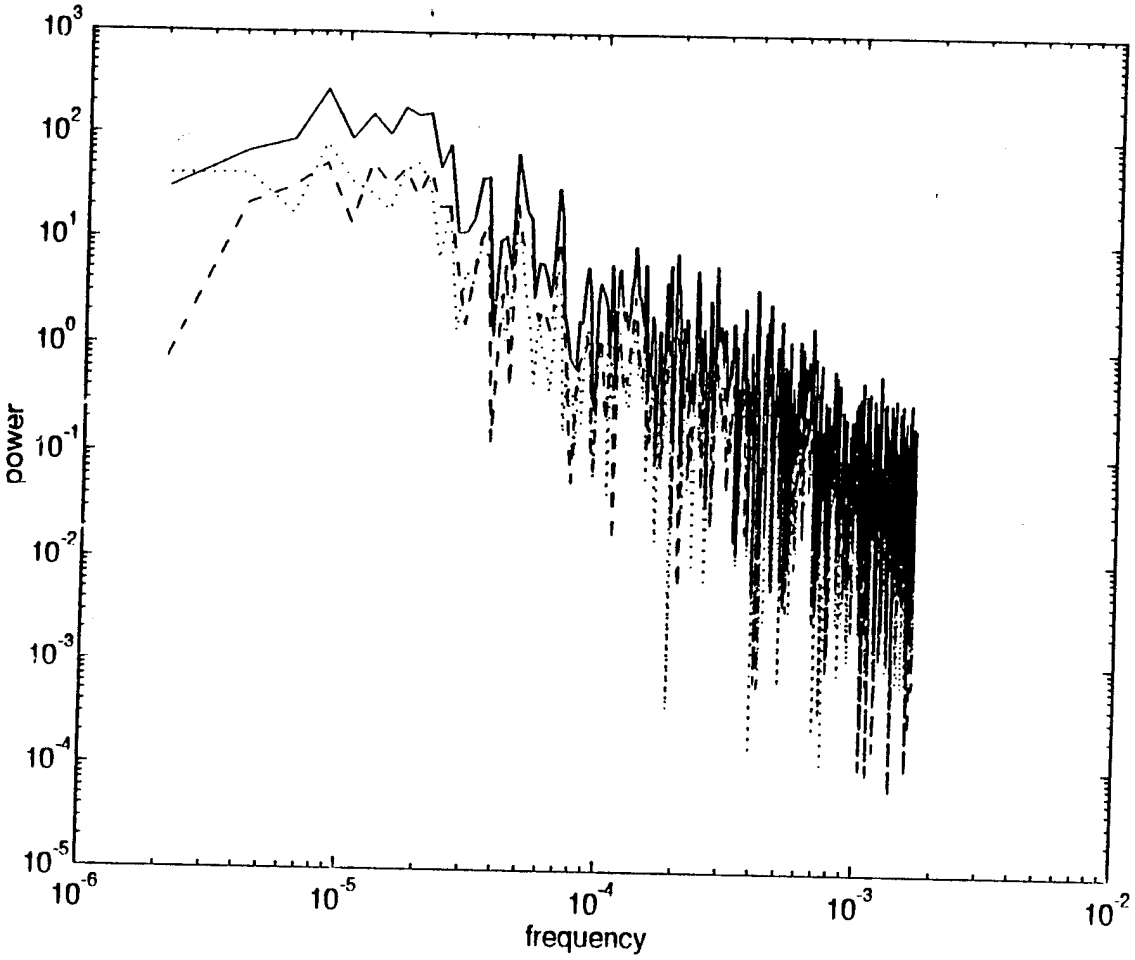

Figure 5.15 Power spectral density of sensible (dotted line), latent (dashed line) and total turbulent (solid line) heat flux (W/m^2) for NORCSEX88 in the Norwegian Sea, March 1988.

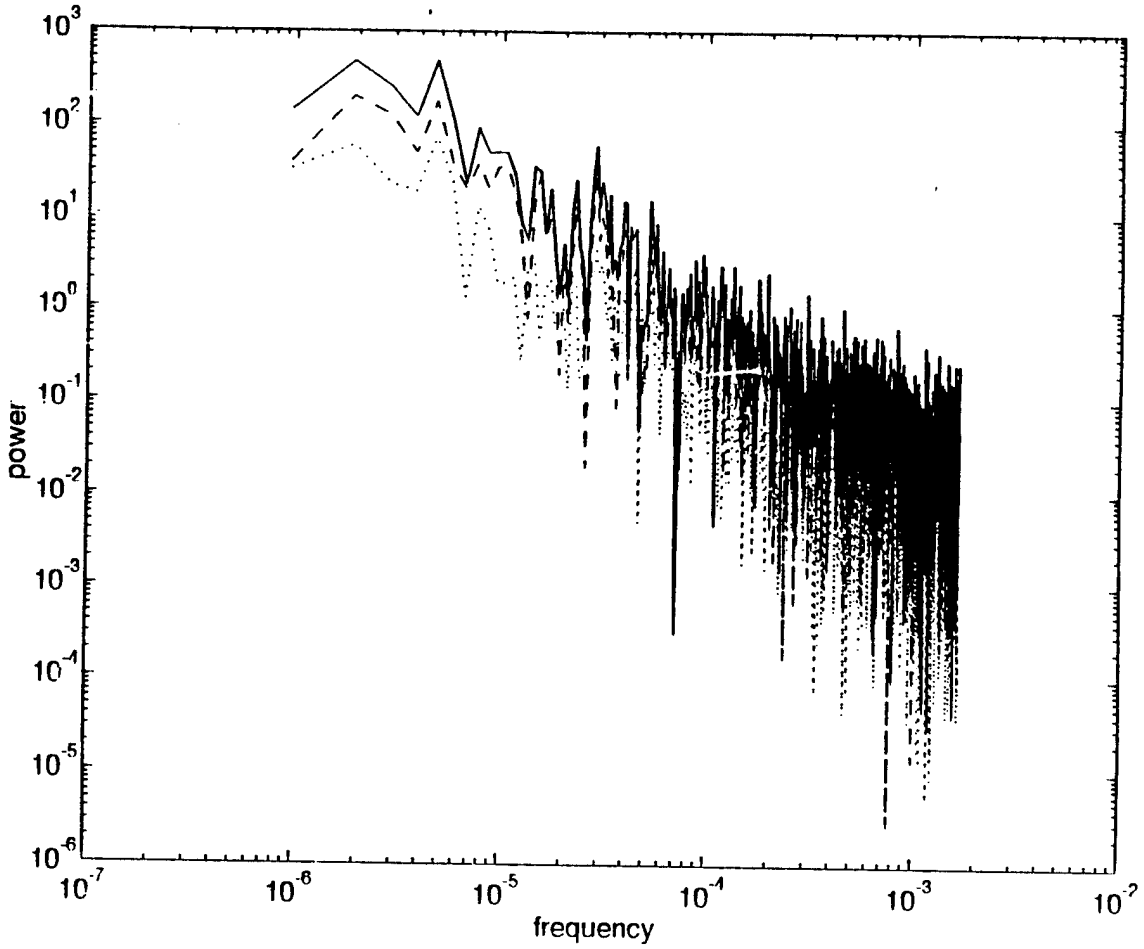

Figure 5.16 Power spectral density of sensible (dotted line), latent (dashed line) and total turbulent (solid line) heat flux (W/m^2) for NORCSEX91 in the Norwegian Sea, November 1991.

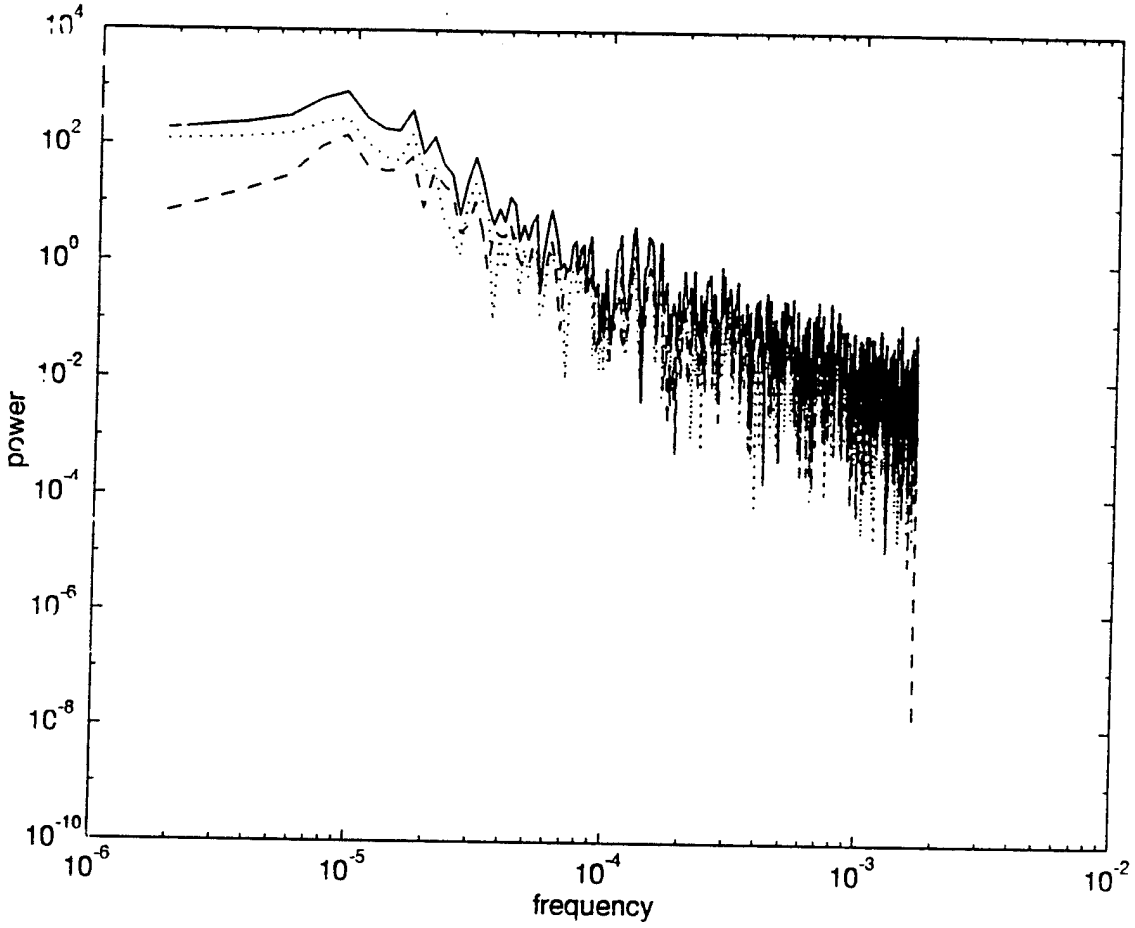

Figure 5.17 Power spectral density of sensible (dotted line), latent (dashed line) and total turbulent (solid line) heat flux (W/m^2) for CEAREX in the Barents Sea, February-March 1989.

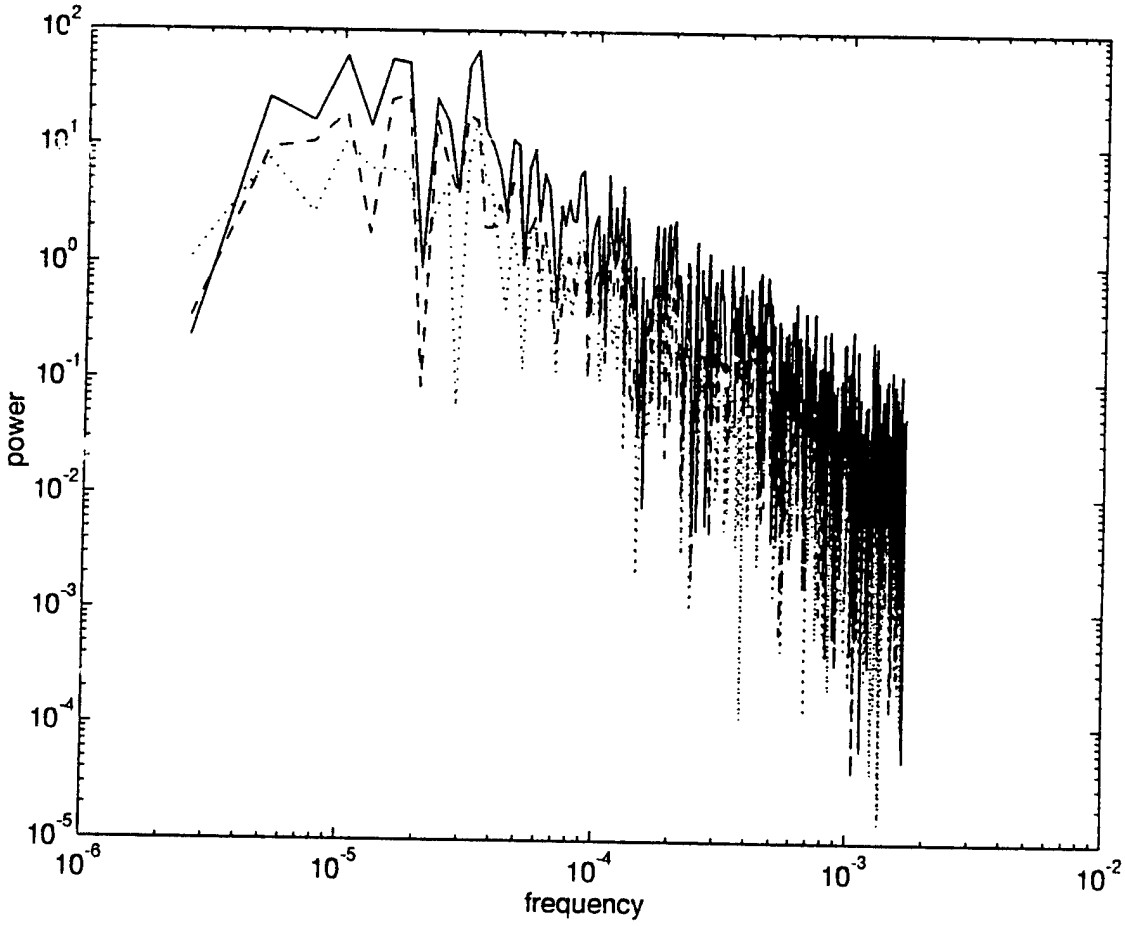

Figure 5.18 Power spectral density of sensible (dotted line), latent (dashed line) and total turbulent (solid line) heat flux (W/m^2) for SIZEX in the Barents Sea, March 1992.

VI. CONCLUSIONS

This thesis examined the exchange of heat between the ocean and atmosphere in the Greenland, Norwegian and Barents Seas. The bulk method was used to calculate the turbulent heat fluxes in the winter based on bulk data gathered aboard ships. The results showed the largest positive fluxes occurring in the Greenland Sea, followed by the Norwegian Sea and the smallest fluxes in the Barents Sea. The Greenland Sea is also a location of strong convective overturning and deep water formation in the Arctic.

The values of the turbulent heat flux were generally found to be consistent with previous climatological results. However, HC flux estimates in proximity to the ice edge were much larger than those observed during the NPS cruises. Specifically, they estimated mean turbulent heat fluxes well in excess of 400 W/m^2 and even as high as 600 to 700 W/m^2 in portions of the Greenland and Barents Seas. Based on the NPS data and in comparison to the climatological works in the regions, the estimates of HC are extremely high. In fact their mean values for some regions of the Greenland and Barents Seas are nearly equivalent to maximum fluxes found in this study. Differences in their heat flux values and those in this thesis may be due in part to larger winds in the HC data. Also, HC used moisture and heat exchange coefficients about 11% and 33% larger than our measured coefficients, explaining some of the differences.

A large uncertainty in the flux measurements of Bunker and HC resulted from the use of questionable heat and moisture exchange coefficients. Bunker used a stability and wind dependent exchange coefficients that appeared to give values about 40% larger than for the method of Smith (1988).

HC used constant exchange coefficients that would be 11-33% larger than those of Smith (1988) for the NPS data sets used in this thesis.

Finally, the averaged values of the bulk meteorological parameters can be used in the bulk formula to obtain averaged sensible and latent heat fluxes within 5% of the actual values. These results validate the classical monthly averaged method (SAM) employed by VT, Gorshkov and others in the Arctic Seas. However, other errors in their method may cause inaccurate results. A principal advantage of the classical method is speed of processing. After the raw data has been quality controlled, an average heat flux can be computed in seconds via the classical method compared with one hour or more with the sampling method.

APPENDIX. [MATLAB PROGRAM FOR COMPUTING HEAT FLUX]

```
% matlab 4.0 program run.m
%  updated Feb 1995
%  based on smith (jgr,v 93,n0 c12, 15467-15472, 1988)
%  calculate the following fluxes
%       shf    sensible heat flux
%       lhf    latent heat flux
%       hf     (total) heat flux
%  based on
%       rho    atm denstiy based on sfc temp
%       ustar  see below
%       tstar  see below
%       l_v    specific heat set constant at 1004 j kg-1 k-1
%      c_p    latent heat of vaporiz const at 2.50e+6 j kg-1
%%%%%%%%%%%%%%%%%%%%%%%%%%%%%%%%%%%%%%%%%%%%%%%%%%%%%%%%%%%%%%%%%%%%%%%%%%%%
zu=15.; %
zt=15.; %
   load norx88;
    myfile=norx88;
[n m]=size(myfile);
for j=1:n;
  min(j) = (j-1) * 10;
  date(j)=myfile(j,1) ;
  time(j)=myfile(j,2);
  utrue(j)=myfile(j,7);
  tair(j)=myfile(j,3);
  tsfc(j)=myfile(j,4);
  rh(j)=myfile(j,5);
  p(j)=myfile(j,6);
  wdt(j)=myfile(j,8);
  lat(j)=myfile(j,9);
  lon(j)=myfile(j,10);
  jd(j) =  67 + (1200 / 1440)  + ( min(j) / 1440);
  wind(j)=utrue(j);
  astd(j)=tair(j)-tsfc(j);
  press(j)=p(j);
  relhum(j)=rh(j);
  sst(j)=tsfc(j);
  temp(j)=tair(j);
  utrue=utrue(j);
  tair=tair(j);
  tsfc=tsfc(j);
  rh=rh(j);
  p=p(j);
%   calculate bulk ustar,tstar,qstar
%  input:  utrue   wind speed (m/s) at zu
%          tair    air temperature (centigrade) at zt
%          rh      relative humidity (%) at zt
```

```
%          tsfc    surface temperature (centigrade)
%          zu      measurement level of utrue (centigrade)
%          zt      measurement level of tair and rh (m)
%          p       atmospheric pressure at zt (mb)
%  output:
%          ustar   friction velocity (m/s)
%          tstar   scaling temperature (k or c)
%        qstar scaling specific humidity (g/kg) not (g/g)!
%          l       monin-obukov length scale (m)
%  calculates tstar based on a constant chn,cen
%  zo base on charnocks relation
%  this follows smith(1988) as close as psby except different
%  virtual temperature calculation is used (smith was wrong)
%  the surface is assumed to be saturated.
%  set constants
  z10=10;      %! reference height (not measuremement height)
% next two are based on value at z10
  ctn=1.0e-3;   %! heat and buoyancy flux xfer param at z10
  cen=1.2e-3;    %! humidity flux transfer parameter
  k=.4;          %! von karmen's constant
  g=9.8;         %! gravity
  a=0.011;       %! charnocks's constant from smith(1980)
  b=0.11;        %! smooth flow constant from businger(1973)
  nu=1.4e-5;     %! dynamic viscosity of air
  gamma=0.0096;  %! adiabatic lapse rate
%%%%%%%%%%%%%%%%%%%%%%%%%%%%%%%%%%%%%%%%%%%%%%%%%%%%%%%%%%%%%%%%%%%%%%%%%%%%
%  calculate parameters not requiring iteration
%  calculate saturation mixing ratio, qsat (g/kg),
%  based on temperature (c) and press (mb) from stull (1988)
%  it is only valid near the surface.use loew's polynomial for
%  more accurate or upper level estimates of qsat.
  psfc=p+0.116 * zt;  % sfc press (mb) based on standard atms
  es=6.1078*exp(17.2694 *tsfc/ (tsfc+237.3));% vap p(mb) tsfc
  qsat=622.0 * es/ (psfc-es);                    % (g/kg)
  esa=6.1078*exp(17.2694 *tair/ (tair+237.3));%vap p(mb) tsfc
  qair=622.0 * esa/ (p-esa);                     % (g/kg)
  q=qair * rh/100; % mixing ratio at zt  (g/kg)
  qsfc=qsat;  %! mixing ratio at surface assumed staturated
  theta=tair+273.16+gamma * zt; %! potent temp (k) at zt
%  the following is based on stull(1988);smith(1988) is wrong
  thetav=theta*(1.0+0.61e-3*q); %! virt potent temp (k) at zt
  tvsfc=(tsfc+273.16)*(1.0+0.61e-3*qsfc);% virt pot temp sfc
%%%%%%%%%%%%%%%%%%%%%%%%%%%%%%%%%%%%%%%%%%%%%%%%%%%%%%%%%%%%%%%%%%%%%%%%%%%%
%  initialization  (these values will change)
  count=0;
  l=1.0e10;
  zo=1.0e-4;
  ustar=utrue * .036;
%  find ustar, tstar loop; exit after convergence or 40 cycles
```

```
%  count is var for the iterations
  if utrue > 0.2;
%  calculate an init ustar
    ustar1=ustar;
    zul = zu / l;
    ztl = zt / l;
    ratio = zu / zo;
%  calculate the integral diabatic heating term
%  for momentum. we have used values from dyer(1974)
%  unstable
    if zu/l < 0.;
      x=(1.-16.*(zu/l))^.25;
psim=2.*logm((1.+x)/2.)+logm((1.+x*x)/2)-2*atan(x)+3.14159/2;
%  stable
    else
      psim = -5 * (zu/ l);
    end
%  for temperature.  based on large and pond (jpo v. 12,1982)
%  unstable
      if zu/l < 0.;
        x=(1.-16.*(zu/l))^.25;
        psit=2.*logm((1.+x*x)/2);
%  stable
      else
        psit = -5 * (zu/ l );
      end
      if ratio < 5.0 ; % prevent underflow
        count=40;
      end
      zot=z10*exp(-k*k / (ctn * logm (zu/zo)));  %
      tstarv= (thetav-tvsfc) * k / (logm(zt / zot)-psit);
      ustar=utrue* k / (logm (zu / zo)-psim);
      zc=a * ustar* ustar/g;                % charnocks formula
      zs =b*nu / ustar;                     % smooth formula
      zo=zc+zs;
      if  abs(tstarv) < 1.0e-20;
        l=1.0e10;
      else
        l=ustar* ustar* tvsfc/ (g*k * tstarv);
      end
% do iterations to find ustar convergence
      if abs((ustar-ustar1)/ustar) > .0005;
        for i=1:40;
        ustar1=ustar;
        zul = zu / l;
        ztl = zt / l;
        ratio = zu / zo;
% this function calculates the integral diabatic heating term
%  for momentum. we have used values from dyer(1974)
```

```
%  unstable
        if zu/l < 0.;
          x=(1.-16.*(zu/l))^.25;

psim=2.*logm((1.+x)/2.)+logm((1.+x*x)/2)-2*atan(x)+3.14159/2;
%  stable
        else
          psim = -5 * (zu/ l);
        end
%  for temperature.  based on large and pond (jpo v. 12,1982)
%  unstable
        if zu/l < 0.;
          x=(1.-16.*(zu/l))^.25;
          psit=2.*logm((1.+x*x)/2);
%  stable
        else
          psit = -5 * (zu/ l );
        end
        if ratio < 5.0 ; % prevent underflow
           count=40;
        end
        zot=z10*exp(-k*k / (ctn * logm (zu/zo)));  %
        tstarv= (thetav-tvsfc) * k / (logm(zt / zot)-psit);
        ustar=utrue* k / (logm (zu / zo)-psim);
        zc=a * ustar* ustar/g;            % charnocks formula
        zs =b*nu / ustar;                  % smooth formula
        zo=zc+zs;
        if  abs(tstarv) < 1.0e-20;
          l=1.0e10;
        else
          l=ustar* ustar* tvsfc/ (g*k * tstarv);
        end
      end % is for i at 40
    end % for abs (  ) >
  end % when u<.2
%           post loop calculations
  if count < 40 & abs((ustar-ustar1)/ustar) < .0005;
    tstar=(tair-tsfc) * k / (logm(zt/ zot)-psit);
    qstar=(q-qsfc) *k / (logm(zt/ zot)-psit);
  else % too stable loop does not converge
    ustar=0.;
    tstar=0.;
    qstar=0.;
    l=0.;
  end
  rho=psfc/(2.87*tvsfc); % calc var density with ideal gas law
  shf(j)=-rho*1004 * ustar* tstar;
  lhf(j)=-rho*2.5e6 * ustar* qstar/1000;1000
  hf(j)=shf(j)+lhf(j);
```

```
  cd(j)=(uustar(j)/ utrue) ^ 2;
  cdn(j)= (1 / sqrt(cd(j))+psim/.4) ^ (-2);
  fprintf('working on observation number %g\n',j)
end %% stop counting j here
```

LIST OF REFERENCES

Blanc, T.V. 1985: Variation of Bulk-Derived Surface Flux, Stability, and Roughness Results Due to the Use of Different Transfer Coefficient Schemes. *J. Phys. Oceanogr.*, 15, 650-669.

Blanc, T.V. 1987: Accuracy of Bulk-Method-Deteremined Flux, Stability, and Sea Surface Roughness. *J. Geophys. Res.*, 92, 3867-3876.

Bourke, R.H. 1994: Class Notes from Polar Oceanography.

British Meteorological Office 1959: Monthly Meteorological Charts and Sea Surface Current Charts of the Greenland and Baretns Seas. Met. Off. Marine Branch, London.

Bunker, A.F. 1976: Computations of Surface Energy Flux and Annual Air-Sea interaction cycles of the North Atlantic Ocean. *Monthly Weather Review,* 104, 1122-1140.

Esbensen, S.K., and R.W. Reynolds 1981: Estimating Monthly Averaged Air-Sea Transfers of Heat and Momentum Using the Bulk Aerodynamic Method. *J. Phys. Oceanogr.*, 15, 650-669.

Gorshkov, S.G. (ed) 1983: *World Ocean Atlas Vol 3 Arctic Ocean,* Pergamon Press, 184 pp.

Hakkinen, S., and D.J. Cavalieri. 1989: A Study of Oceanic Heat Fluxes in the Greenland, Norwegian, and Barents Seas. *J. Geophys. Res.*, 94, 6145-6157.

Hanawa, K., and Y. Toba. 1987: Critical Examination of Estimation Methods of Long-Term Mean Air-Sea Heat and Momentum Transfers. *Ocean-Air Interactions,* 1, 79-93.

Kaimal J.C. and J.J. Finnigan, 1994: *Atmospheric Boundary Layer Flows.* Oxford University Press, New York, NY 289 pp.

Ledvina, D.V., G.S. Young, R.A. Miller, and C.W. Fairall. 1993: The Effect of Averaging on Bulk Estimates of Heat and Momentum Fluxes for the Tropical Western Pacific Ocean. *J. Geophys. Res.*, 98, 20211-20217.

Lumley, J.L., and H.A. Panofsky, 1964: *The Structure of Atmospheric Turbulence.* Wiley-Interscience, New York, 239 pp.

Smith, S.D. 1988: Coefficients for Sea Surface Wind Stress, Heat Flux, and Wind Profiles as as Function of Wind Speed and Temperature. *J. Geophys. Res.*, 93, 15467-15472.

Sverdrup, H.U. 1951: Evaporation from the Oceans. *Comp. of Met. Am. Met. Soc.* 1071-1081.

Swift, J.H., T. Takahashi, and H.D. Livingston, 1983: The Contribution of the Greenland and Barents Seas to the Deep Water of the Arctic Ocean. *J. Geophy. Res.*, 88 5981-5986.

Vowinckel, E. and B. Taylor, 1964: Evaporation and Sensible Heat Flux over the Arctic Ocean. Air Force Cambridge Research Laboratories, United States Air Force, Bedford, MA, Report No. AFCRL-64-272.

INITIAL DISTRIBUTION LIST

1. Defense Technical Information Center 2
   Cameron Station
   Alexandria, VA 22304-6145

2. Library, Code 52 2
   Naval Postgraduate School
   Monterey, CA 93943-5101

3. Oceanography Department 1
   Code OC/BF
   Naval Postgraduate School
   Monterey, CA 93943-5122

4. Meteorology Department 1
   Code MR/HY
   Naval Postgraduate School
   Monterey, CA 93943-5114

5. Peter S. Guest 1
   Code MR/GS
   Naval Postgraduate School
   Monterey, CA 93943-5114

6. Roland W. Garwood 1
   Code OC/GD
   Naval Postgraduate School
   Monterey, Ca 93943-5122

7. Arlene Guest 1
   Code OC/GT
   Naval Postgraduate School
   Monterey, CA 93943-5122